Coordination Chemistry Reviews 254 (2010) 1101–1116

Contents lists available at ScienceDirect

Coordination Chemistry Reviews

journal homepage: www.elsevier.com/locate/ccr

Review

Chemical functionalization of single-walled carbon nanotube field-effect transistors as switches and sensors

Song Liu [a], Qian Shen [a], Yang Cao [a], Lin Gan [a], Zhenxing Wang [a], Michael L. Steigerwald [b], Xuefeng Guo [a,*]

[a] Beijing National Laboratory for Molecular Sciences (BNLMS), State Key Laboratory for Structural Chemistry of Unstable and Stable Species, College of Chemistry and Molecular Engineering, Peking University, Beijing 100871, PR China
[b] Department of Chemistry and the Columbia University Center for Electronics of Molecular Nanostructures, Columbia University, New York, New York 10027, United States

Contents

ARTICLE INFO

Article history:
Received 25 August 2009
Accepted 8 November 2009
Available online 11 November 2009

Keywords:
Single-walled carbon nanotube
Chemical functionalization
Self-assembly
Micro/nanofabrication
Optoelectronic devices

ABSTRACT

Because of the one-dimensional (1D) nanostructural nature of single-walled carbon nanotubes (SWNTs) and their advantages of chemical flexibility and sensitivity arising from the susceptibility of their active surfaces to interacting species, great effort has been made to integrate carbon nanotube field-effect transistors (NTFETs) into functional optoelectronic devices capable of converting external stimuli to easily detectable electrical signals. In this *Review* article, we aim to capture recent advances of rational design and chemical functionalization of NTFETs for the purpose of switching or biosensing applications. To provide a deeper understanding of the device responses to analytes, this review will also survey the proposed sensing mechanisms. As demonstrated by these remarkable examples, the concept of combining the proper selection of functional molecular materials and molecular self-assembly with device micro/nanofabrication offers attractive new prospects for constructing NTFET-based molecular optoelectronic devices with desired functionalities.

1. Introduction

The functionalization of nanoscale materials with functional molecular materials with desired properties is an important tool for mimicking functions of biological systems such as vision and photosynthesis, ensuring the conversion of external inputs to useful signals for information processing [1–11]. In particular, the integration of 1D nanomaterials, such as nanowires and nanotubes, into functional electronic devices has received considerable attention in the fields of microelectronics and nanoelectronics due to their potential applications in switching, detecting and sensing systems [6,11–21]. 1D nanomaterials are good can-

* Corresponding author. Tel.: +86 10 62757789; fax: +86 10 62757789.
E-mail address: guoxf@pku.edu.cn (X. Guo).

0010-8545/$ – see front matter © 2009 Elsevier B.V. All rights reserved.
doi:10.1016/j.ccr.2009.11.007

didates for switching and sensing because of their reduced low-dimensionality. For example, shrinking the dimensions of the materials down to the nanometer scale can strengthen the important role of surface chemistry of the materials since they are comparable in size to the analytes detected. On the other hand, the low-dimensionality also produces ultraminiaturized structures with exceptionally large surface-to-volume ratio. The synergistic effect of the two aspects resulting from the reduced size affords a unique class of materials that has the intrinsic ultrasensitivity towards changes in their local chemical environment. In addition to that, shrinking the dimensions of the devices down to the nanoscale also meets the ever-increasing requirements of the scaling of conventional silicon-based complementary metal-oxide semiconducting technology (CMOS) in industry [5,22,23]. Therefore, it is of crucial importance to develop nanomaterials and paradigms for device architecture and operation to install functionality into devices capable of converting an external stimulus to an easily detectable electrical signal.

Since their discovery in 1991 by Ijima [24], carbon nanotubes have been regarded as one of the best nanostructural materials derived from bottom-up chemical synthesis approaches. Carbon nanotubes have the simplest chemical composition and atomic bonding configuration but exhibit perhaps the most extreme diversity and richness among nanomaterials in structures and structure–property relations [1,2]. The structure of single-walled carbon nanotubes (SWNTs) can be appreciated by folding up a graphene sheet into a cylinder along a certain lattice vector. This hints at useful conduction via the π-bonding network. Each atom on the surface of SWNTs is exposed to the environment and, thus, any small changes from their environment could cause drastic changes in their electrical properties. Moreover, depending on the chirality and diameter, SWNTs can be either metallic or semiconducting. This suggests different energy band alignment scenarios between SWNTs and interacting molecules. These can be expected to yield a useful variety of device properties. Another significant feature of SWNTs is that they are one-dimensional ballistically-conducting nanowires that are intrinsically the same size as the molecules. They are long enough and can be easily micro/nanofabricated on a large range of substrates. Ultimately, SWNTs are molecular chemicals entirely composed of carbon atoms, which provide a natural match to organic molecules, and also allow us, to an extent, to tailor their chemical reactivity. As a result of all of these features, SWNTs have great potential for switching and sensing applications.

The first nanotube field-effect transistors (NTFETs) were independently obtained in 1998 from both the Dekker group at Delft University and the Avouris group at IBM [25,26]. These two reports led to a deluge of worldwide research interest in carbon nanotube electronics due to their potential in applications in areas as varied as switching, sensing, molecular electronics, gas storage, field emission devices, drug discovery, catalyst supports, probes for scanning probe microscopy, and components in high-performance composites. The main focus of this *Review* article is to summarize recent progresses in the design, fabrication, and electrical properties of functional molecular devices based on NTFETs for switching and sensing applications in the past few years. The design principle is the combination of the proper selection of molecular materials and molecular self-assembly with micro/nanofabrication to construct functional optoelectronic devices. However, this research field is a diverse and rapidly growing one. Having limited space and references, we will only be able to cover some of the major contributions with the most general applicability and highlight some important aspects, which were neglected in most previous reviews. Fortunately, there are a number of excellent previous review papers in the literature covering various aspects of carbon nanotube electronics, which can amend these deficiencies [1–3,5,11,17–19,27–35].

2. Functionalization strategies

Many applications based on SWNTs require chemical functionalization of the carbon nanotubes to make them more amenable to rational and predictable manipulation because the insolubility of SWNTs in most organic solvents and the difficulties of dealing with these highly intractable carbon nanostructures restrict real-life applications of SWNTs to a considerable extent. To improve the properties of SWNTs, two generalized approaches to achieve the desired results involve covalent and non-covalent modification of SWNT sidewalls. In terms of covalent modification, one convenient approach is to oxidize the SWNT sidewalls to nanotube-bound carboxylic acids [36–47]. SWNTs, after functionalization with carboxylic acid groups, can undergo further modification with a range of organic entities by means of amide/ester linkages or carboxylate-ammonium salt ionic interactions (Fig. 1A) [36–45]. Another popular method for the covalent functionalization of SWNTs is the fluorination of SWNTs because the SWNT sidewalls are expected to be inert [46,47]. The fluorine atoms in the fluorinated SWNTs can be substituted by alkyl groups through treatment with carbon anions, such as alkyl lithium or Grignard reagents (Fig. 1A). Although covalent modifications are often effective at installing functionality, they result in a change of carbon hybridization from sp^2 to sp^3, potentially leading to a partial impairment of conjugation with consequences for mechanical and/or electron-transport properties of SWNTs. Non-covalent functionalization [11,18,19,48–51], on the other hand, not only improves the solubility of SWNTs in solvents but also constitute invasive processes, preserving the primary structures of SWNTs along with their unique electronic and mechanical properties. It is because of these reasons that non-covalent functionalization has been extensively used to build functional optoelectronic devices. In general, there are two main schemes to non-covalent functionalization of SWNT sidewalls (Fig. 1B). The first approach employs functional aromatic compounds that exhibit π–π stacking on the sidewalls of SWNTs. For example, a pyrene headgroup [49–51], commonly used for graphite functionalization, is typically utilized as an anchor for non-covalent functionalization. The second type of non-covalent functionalization is to use long alkyl chain, surfactants, biomacromolecules, and polymers through hydrophobic interactions [18,19,48,52]. It is believed that in most cases the mode of interaction between SWNTs and these components are helical wrapping or simple surface adsorption [53–66]. For example, SWNTs can be made water-soluble by wrapping in amylase (linear component of starch) [56]. After starch functionalization, NTFETs were used to detect the catalytic activity of the enzyme, α-amylase, which can break starch down into smaller carbohydrate fragments, such as glucose [67].

3. Sensing mechanisms

Depending on the chirality and diameter, SWNTs can be either metallic or semiconducting [68]. Semiconducting SWNTs can be used to fabricate FET devices, which can operate at room temperature and in ambient conditions [25,26]. In a standard NTFET, a semiconducting SWNT is connected to metal source and drain electrodes through which a current is injected and collected, respectively (Fig. 2). The conductance of the devices between the source and the drain is switched on and off by a third gate electrode that is capacitively coupled through a thin dielectric layer. In the case of a p-type SWNT, applying a positive gate voltage depletes carriers and reduces the conductance, whereas applying

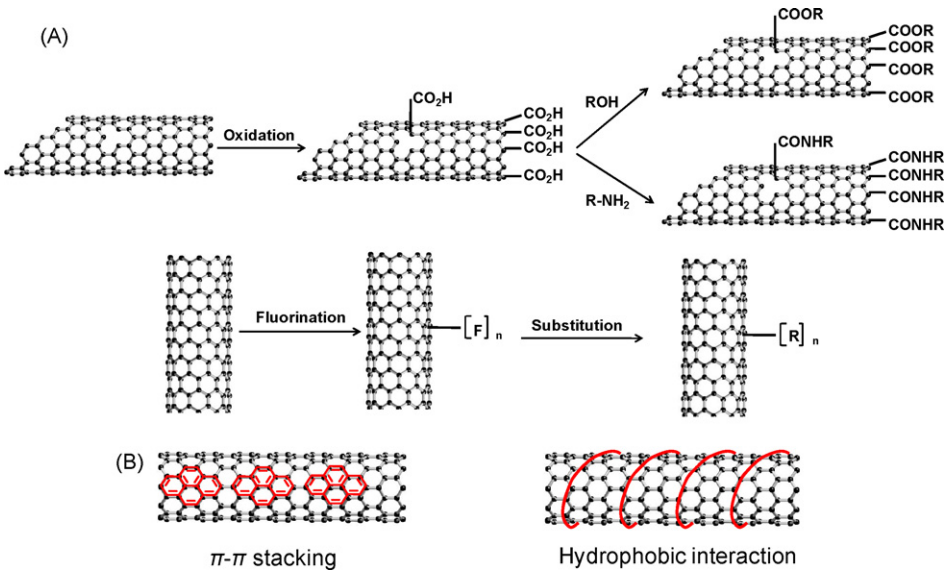

Fig. 1. Schematic presentation of functionalization strategies of SWNT sidewalls: covalent functionalization (A) and non-covalent functionalization (B).

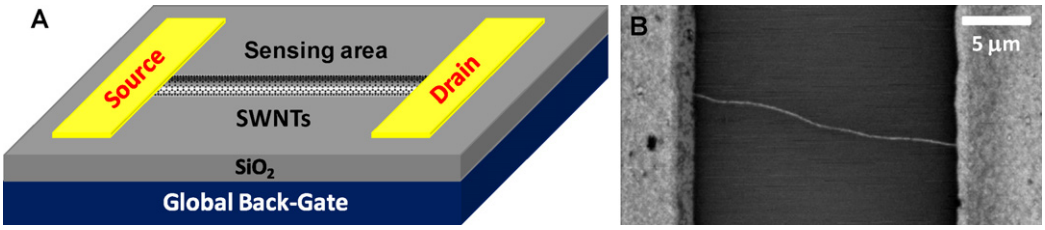

Fig. 2. (A) Schematic representation of a NTFET device. (B) A representative scanning electron micrograph (SEM) of an individual straight SWNT spanning source and drain electrodes on a silicon oxide surface.

a negative gate voltage leads to an accumulation of carriers and increases the conductance. The gate-dependence of the conductance of NTFETs makes them natural candidates for electrically based sensing because the electric field resulting from the changes in the local environment to the gate dielectric is analogous to the effect of applying a voltage with a gate electrode. Since each atom on the surface of SWNTs is exposed to the environment, any small changes from their environment could cause drastic changes to their electrical properties. After the interactions between analytes and SWNTs, charge transfer might occur from analyte molecules to the carbon nanotubes, potentially leading to the shift of the threshold voltages to either more negative values (if the analytes are electron-donating), or more positive values (if the analytes are electron-withdrawing). On the other hand, the analytes could also generate a scattering potential across the carbon nanotubes. In this case, the overall conductance of the devices will decrease because of the scattering effect produced by the target analytes adsorbed on the surface of SWNTs. In some cases, the devices used for chemical and biological sensing have carbon nanotubes and nanotube-metal contacts directly exposed to the environment. The changes in conductance of this type of devices could be dominantly caused by the interplay between molecules and metal contacts or contact interfaces. The adsorbed analytes could change the work function of the exposed portion of metal contacts and thus the Schottky barrier between nanotubes and metal electrodes [50,69–75]. Through this mechanism, NTFETs were used to detect specific protein–protein interaction at 1 pM concentrations by increasing the Schottky contact area [71]. However, the exact sensing mechanism of NTFET-based sensors is still a topic of debate. It is logically very difficult to separate the behavior of the contacts or contact interfaces from the interactions between nanotubes and analytes, since the operating devices must be a combination of all of them [76,77]. More discussion can be found in Section 6.

4. Organic materials-functionalized NTFET devices

Organic materials, such as long alkyl chain, pyrene, porphyrin, polymer, and their derivatives, do interact with the sidewalls of SWNTs by means of π–π stacking and hydrophobic interactions, thus opening up the way for non-covalently functionalizing SWNTs. Their attractive feature is that when tethered on the surfaces of SWNTs, these organic materials, with the opportunities open to their wide-ranging functionalities, such as electromechanical, photochromic, optical, molecular recognition, and magnetic behaviors, might lead to novel devices that show interesting properties of switching and sensing.

4.1. Catenane-functionalized switches

Catenanes are a family of mechanically-interlocked molecules with one or more rings encircling a dumbbell-shaped component (Fig. 3). As prime candidates for the construction of artificial molecular machines, catenanes have become the subject of intense investigation [78–83]. Among rotaxanes, [2]catenanes contain two recognition sites and one cyclic moiety, which encircles either of the two recognition sites (Fig. 3). One important feature of [2]catenanes is that the cyclic moiety can be mechanically switched between the two stations upon external stimuli, such as redox reactions and light irradiation [84]. By employing this property, the Stoddart group has demonstrated that, for particular device configurations, these bistable molecules can be utilized as

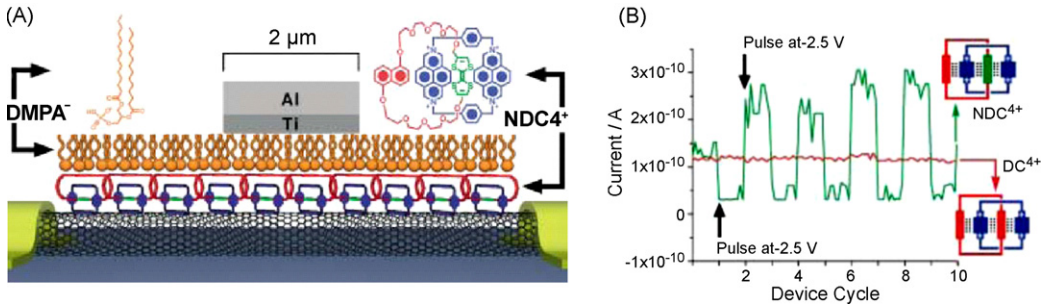

Fig. 3. (A) A schematic representation of an SWNT—STJ device. (B) Device cycling for the nondegenerate [2]catenane (green) contrasted with the lack of cycling for the degenerate [2]catenane (red). These graphics are reproduced from ref. [87] with permission from the copyright holder.

solid-state voltage-addressable, nonvolatile switches that operate reversibly under ambient conditions [84–86]. Another recent interesting result from the same group is the design and fabrication of SWNT hybrid-based molecular switch tunnel junctions (MSTJs) [87]. In this report, they described two-terminal MSTJs that incorporate a semiconducting SWNT as the bottom electrode (Fig. 3). A high-quality Langmuir-Blodgett monolayer of bistable, nondegenerate [2]catenane tetracations, self-organized by their supporting amphiphilic dimyristoylphosphatidyl anions, which shield the mechanically switchable tetracations from a 2 μm-wide metallic top electrode, were non-covalently coated on the surface of SWNTs. This passivation strategy proved to be efficient so as to avoid electrical shorts between the top and bottom electrodes. The resulting 0.002 μm^2 area tunnel junction addresses a nanometer-wide row of ca. 2000 molecules. Current–voltage measurements demonstrated that these devices can be switched reconfigurably and cycled repeatedly between high- and low-current states under ambient conditions (Fig. 3). Control experiments, using a closely related nondegenerate [2]catenane, yielded no similar signatures, either in the solution phase or in devices. These results have implications of the design of molecular electronic devices, such as the precise choice of functional molecular materials and electrode materials.

4.2. Photochromism-functionalized switches

Photochromic molecules, such as spiropyrans, diazobenzenes, and their derivatives [88,89], can undergo reversible structural interconversions and modulation of photophysical properties upon exposure to external optical, chemical, or thermal stimulations, thus constituting a family of promising nanobuilding blocks of great importance for designing and constructing functional molecular devices. Among them, particular attention is paid to photochromic spiropyrans because they can toggle back-and-forth between a neutral, colorless form and a zwitterionic, colored form. The charge-separated ring-opened form is generated by illumination with UV light, whereas the reversing ring closure is effected with visible light to form the neutral state. The reversible photoisomerization causes a significant change in the electric dipole moment of the molecule. Such a change in dipole moment could initiate a significant change in the electrostatic environment. This photoinduced electrostatic environment can function as a local negative gate voltage, thus modulating the electrical conductivity in devices. Based on this hypothesis [90–93], we have demonstrated the reversible photomodulation of the electrical conductivity of spiropyran-functionalized pentacene thin films through rubber stamping. Another promising application of spiropyrans is the functionalization of the surfaces of SWNTs through molecular self-assembly to give photosensitive devices [94]. In this study, we synthesized versions of the spiropyrans that were derivatized with either alkane or pyrene groups because these moieties have been shown by Dai and co-workers to non-covalently associate with the surface of carbon nanotubes [49,51]. These functional headgroups acted as anchors to hold the photoswitchable spiropyrans in proximity to the tube surface (Fig. 4). Once the photochromic molecules are tethered to the surfaces of the SWNTs, the device characteristics become very sensitive to light. We found large changes in R_{on} occur in the photochromic NTFET devices when the spiropyrans are photoswitched to their charge-separated merocyanine form (Fig. 4). The reverse process in spiropyrans (i.e., from the charge-separated merocyanine form to the closed spiropyran form) is initiated with visible light. After further exposure to visible light, the device characteristics are essentially restored to the original values before UV irradiation. A Schottky barrier is known to form at these junctions and could, in principle, complicate the analysis [50,69–75]. To eliminate this possibility, we covered the junctions with an insulating layer using hydrogensilsesquioxane resin (HSQ) that was patterned using electron beam lithography. These junction-protected devices were then immersed in solutions of spiropyrans. The electrical properties are essentially the same as that shown in Fig. 4, indicating that the observed photoswitching effect of the molecules tethered on the SWNT is responsible for the change in device characteristics.

To gather kinetic data on this process of devices, we followed the drain current as a function of time while the device is held at 50 mV source-drain bias and −9 V gate bias as the light is toggled between UV and visible wavelengths. From the data in Fig. 5, the forward and reverse rate constants, k (UV) = $1.9 \pm 0.2 \times 10^{-3}$ s^{-1} and k (visible) = $1.5 \pm 0.1 \times 10^{-3}$ s^{-1}, were obtained. The time scale for this process is similar to that measured by Haddon and co-workers [95], but much faster than the rates of switching spiropyrans in the crystalline state [96]. This implies that the spiropyrans are not tightly packed on the tube surface. After the third switching cycle shown in Fig. 5, the device was left in the dark. To revert fully back to the high conductance state takes more than 6 h. This study provides a clear example of how to combine microfabrication with molecular self-assembly to produce field-effect devices that detect the photoswitching events of around 10^4 molecules. At a rudimentary level, these devices accomplish a task similar to biological processes, such as vision and photosynthesis, where light is sensed and converted into a signal.

Following the initial work, Simmons and Zhou et al. used the similar methods to functionalize SWNTs with azobenzene-based chromophores [97,98]. In the Simmons' case [97], an azo-based chromophore with an anthracene tether was utilized to non-covalently functionalize SWNTs for forming an optically active nanotube-hybrid material (Fig. 6A). Upon UV illumination, the conjugated chromophore underwent a *cis-trans* isomerization leading to a charge redistribution near the nanotube. This charge redistribution changes the local electrostatic environment, shifting the threshold voltage and increasing the conductivity of the nanotube transistor. For a 1–2% coverage, they observed a shift in the thresh-

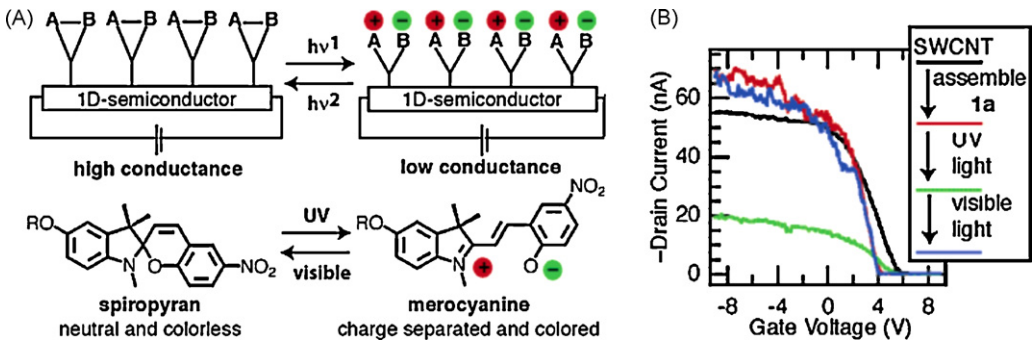

Fig. 4. (A) A one-dimensional semiconductor that has molecules assembled on its surface. Light is used to toggle the molecules between a cyclized (left) and charge-separated (right) state. These molecules contain a SWNT recognition domain and a photoswitchable headgroup (alkyl chain or pyrene). (B) Change in drain current of an individual SWNT device as a function of *Vg*. The source drain bias voltage is held at 50 mV. Black curve is device before assembly; red curve is device after assembly of molecules; green curve after irradiation with UV light for ~10 min; blue curve after irradiation with visible light. These graphics are reproduced from ref. [94] with permission from the copyright holder.

old voltage of up to 1.2 V. The remarkable result they found is that the conductance change was reversible and repeatable over long periods of time, indicating that the chromophore-functionalized nanotubes are useful for integrated nanophotodetectors. In the Zhou's case [98], they reported a nanoscale color detector based on a SWNT functionalized with azobenzene chromophores, where the chromophores serve as photoabsorbers and the nanotube as the electronic read-out (Fig. 6B). By synthesizing chromophores with specific absorption windows in the visible spectrum and anchoring them to the nanotube surface, they demonstrated the controlled detection of visible light of low intensity in narrow ranges of wavelengths. The measurements suggest that upon photoabsorption, the chromophores isomerized from the ground state *trans* configuration to the excited state *cis* configuration, accompanied by a large change in dipole moment, changing the electrostatic environment of the nanotube. In addition, they performed all-electron ab initio calculations to study the chromophore-nanotube hybrids, which showed that the chromophores bind strongly to the nanotubes without disturbing the electronic structure of either species. Calculated values of the dipole moments support the notion of dipole changes as the optical detection mechanism. This system can be used to study fundamental properties of chromophore-nanotube hybrids and to probe molecular transitions.

4.3. Chromophore-functionalized switches

The photophysical properties of photosensitive molecules or polymers make them strong candidates for various demanding

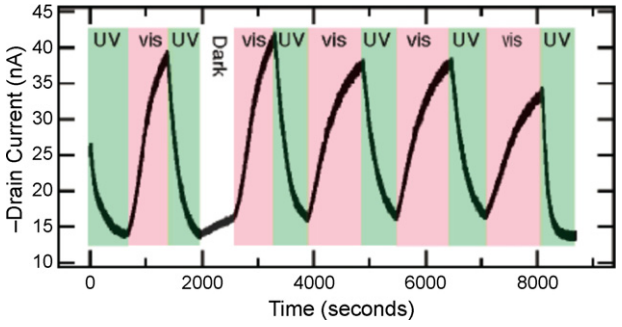

Fig. 5. Time course of the drain current for a SWNT transistor with spiropyrans assembled on its surface. The bias between the source and drain electrodes is 50 mV, and the gate bias is −9 V. Alternating irradiation with UV (365 nm) and visible light (633 nm). After ~2000 s, the device was measured in the dark and found to slowly revert back to the closed form of the spiropyran. This graphic is reproduced from ref. [94] with permission from the copyright holder.

applications [99–102], such as telecommunication, thermal imaging, remote sensing, thermal photovoltaics, light-emitting diode, and solar cells. These materials, when combined with NTFETs, might afford new types of functional optoelectronic devices. For example, prototypes of optoelectronic memory devices based on NTFETs have been reported recently [103–106].

Porphyrin, the light-absorbing chromophore in chlorophyll, plays a central role in photosynthesis because of their long-lived intermediate electronic state under visible light irradiation. The uniqueness of charge-separated states of porphyrin can be used to functionalize NTFETs for mimicking the electron transfer process in nature. By employing a zinc porphyrin derivative [107,108], Hecht et al. fabricated visible light sensitive NTFET switches that directly detected a photoinduced electron transfer (PET) within a donor/acceptor (D/A) system (Fig. 7A). They found that the SWNTs act as the electron donor and the porphyrin molecules as the electron acceptor. The magnitude of the PET was measured to be a function of both the wavelength and intensity of applied light, with a maximum value of 0.37 electrons per porphyrin for light at 420 nm and 100 W/m^2 (Fig. 7B). These results are helpful for understanding the photophysics of this D/A system, which may form the basis for applications in artificial photosynthesis and alternative energy sources such as solar cells.

In another interesting report, Pradhan et al. [109] discovered that rigid, conjugated macromolecules, poly(*p*-phenylene ethynylene)s (PPEs), can be used to non-covalently functionalize SWNTs. After functionalization, the resulting SWNTs were mixed with polycarbonate solution to form a homogeneous SWNT-polycarbonate composite solution, which can be cast on the glass substrate ultimately to form free-standing films. Electrical contacts to the films were made with silver paste. Electrical conductivity measurements indicated that these two-terminal devices were very sensitive to infrared light (Fig. 8A). The conductivity change in a 5 wt% SWNT-polycarbonate nanocomposite is significant (4.26%) and sharp upon infrared illumination in the air at room temperature [110,111]. By comparing with the results in the infrared photoresponse of a pure SWNT film, they concluded that the photoeffect predominated in the infrared photoresponse of SWNT-polycarbonate nanocomposites.

In the similar way, Borghetti et al. [112] used a photoconducting polymer, poly(3-octylthiophene-2,5-diyl) (P3OT) to achieve polymer-functionalized NTFETs (Fig. 8B). The process impacts both the ON- and the OFF-states of the transistor with the change in conductance reaching four orders of magnitude upon illumination. Remarkably they found that depending on the applied gate bias, the device can be optimized as a memory element or as an optical switch (optically driven current modulator). On the

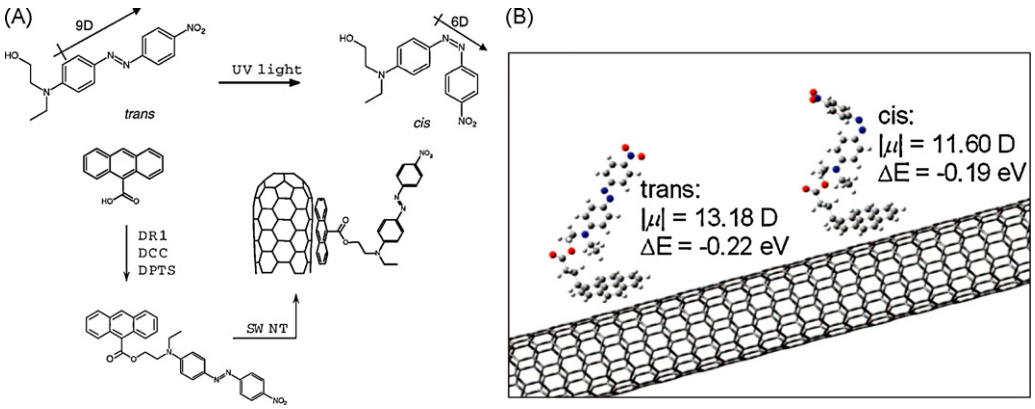

Fig. 6. (A) Under UV light, the azo-based chromophore isomerizes from the equilibrium *trans* conformation to the metastable *cis* conformation. In doing so, the molecular dipole moment changes from 9 to 6 D. (B) Optimized geometries, dipole moments, and binding energies for a pyrene-derivatized nitroazobenzene non-covalently attached to a (10,0) nanotube. The pyrene unit is in contact with the nanotube surface at a distance of about 2.8 Å. These graphics are reproduced from ref. [97] and [98] with permission from the copyright holder.

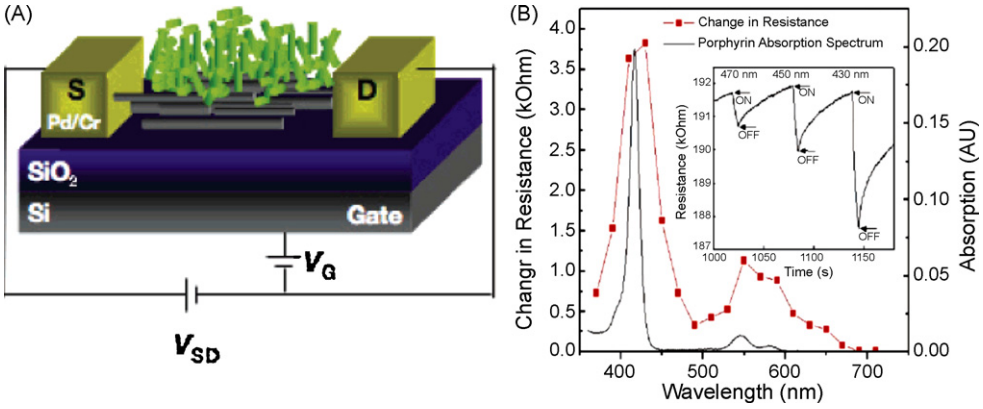

Fig. 7. (A) Schematic of the porphyrin-functionalized device used for transistor measurements. (B) Change in resistance of device coated with porphyrin in response to light of varying wavelengths but constant intensity. The time dependence of the resistance is shown in the inset for three different wavelengths as the light was cycled on and off. The larger graph shows the change in resistance of the device at each wavelength in response to the light being on for 5 s. Also included is the absorption spectrum of the porphyrin molecule. The plot shows a correlation between the porphyrin absorption spectrum and the change in device resistance. These graphics are reproduced from ref. [107] with permission from the copyright holder.

basis of a set of experiments performed with either NTFETs or polymer thin-film transistors (TFTs), they proposed a mechanism based on the trapping of photogenerated electrons at the nanotube/gate dielectric interface. These trapped electrons act as an effective "optical gate" for the nanotube transistor. These results demonstrated that the polymer-functionalized NTFETs, as a very sensitive charge sensor, proved to be a good tool to study the charge distribution and dynamics in polymer thin-film transistors [112,113].

4.4. Molecular recognition-based sensors

Increasing the selectivity, response speed, and sensing ability of devices is one of the key requirements for practical applications in switching, detecting, and sensing systems. To achieve this goal, host–guest chemistry is a powerful strategy of great importance to impart the necessary selectivity for distinguishing the structural isomers and stereoisomers. Based on the concept of molecular recognition, Zhao et al. [114] have fabricated

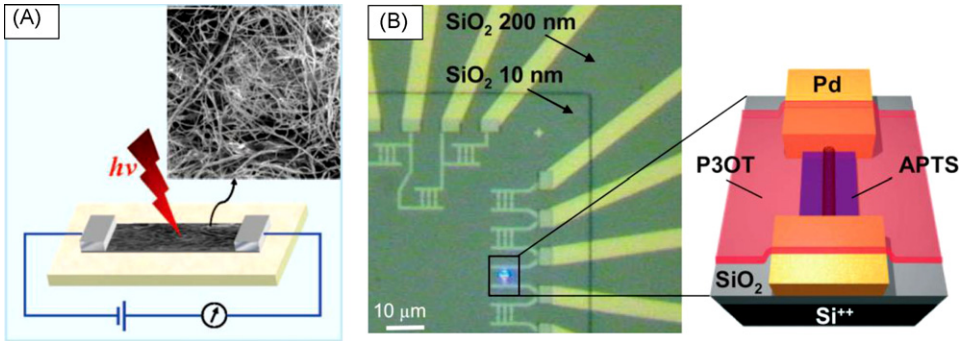

Fig. 8. (A) Schematic experimental setup for detecting infrared light. Inset: SEM image of the 5 wt% SWNT-polycarbonate nanocomposite film (scale bar: 1.0 μm). (B) Optical microscope image of the sample showing a series of self-assembled NTFETs and the blue laser spot focused on an individual transistor. The magnification shows a schematic of the NTFET showing a single nanotube connected by Pd electrodes separated by ca. 100 nm and coated with the P3OT film. These graphics are reproduced from ref. [109] and [112] with permission from the copyright holder.

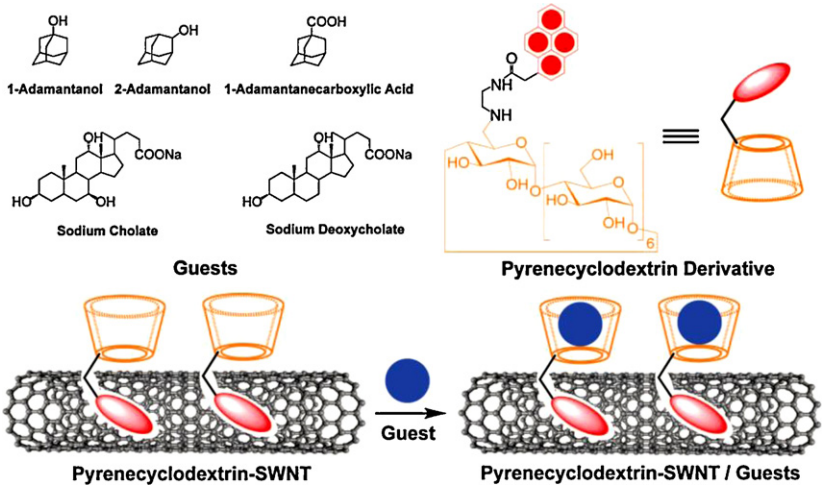

Fig. 9. Schematic representation of the pyrenecyclodextrin-decorated SWNT hybrids. The following sequence of sensing abilities for the guest molecules: 1-Adamantanol, 2-Adamantanol, 1-Adamantanecarboxylic Acid, Sodium Deoxycholate, and Sodium Cholate. The graphic is reproduced from ref. [114] with permission from the copyright holder.

pyrenecyclodextrin-decorated NTFET devices to sense particular organic molecules (Fig. 9). Interestingly, the transistor characteristics of the pyrenecyclodextrin-decorated SWNT/FET device shifted towards negative gate voltage in the presence of certain molecules, some of which are included inside the cavities of cyclodextrins with moderate binding constants, and do not have appreciable interactions with the SWNTs. The magnitudes of the shifts for these organic molecules depend highly on their complex formation constants (K_S) with the pyrenecyclodextrin and follow a linear relationship. The mechanism is postulated to involve either the change of the carrier concentration as a result of the change in the charge transfer from the pyrenecyclodextrins to the SWNTs in the pyrenecyclodextrin-decorated SWNT/FET, or because of the change in the carrier mobility resulting from differences in the scattering potential as a consequence of deformation of the SWNTs. These experimental results indicate that the electrical conductance of the pyrenecyclodextrin-decorated SWNTs is highly sensitive to certain organic molecules and varies significantly with changes in the surface adsorption of these molecules. Thus, the pyrenecyclodextrin-SWNT/FET device can serve as a chemical sensor to detect organic molecules, not only selectively, but also quantitatively, an outcome which augurs well for real-life applications.

Following this initial work, the same group used the same approach to fabricate a tunable photosensor based on pyrenecyclodextrin-decorated NTFET devices to sense a fluorescent adamantyl-modified Ru complex (ADA-Ru) (Fig. 10) [115]. When the light is on ($I = 40\,W\,m^{-2}$ and $\lambda = 280\,nm$), the transfer curve of the pyrenecyclodextrin-NTFET device shifts toward a negative gate voltage by about 1.6 V and its sheet resistance increases quickly, indicating a charge-transfer process from the pyrenecyclodextrins to the SWNTs. On the contrary, the transfer curve of the pyrenecyclodextrin-SWNT/FET device in the presence of the ADA-Ru complex shifts toward a positive gate voltage by about 1.9 V and its sheet resistance decreases slowly when the light is on ($I = 40\,W\,m^{-2}$ and $\lambda = 490\,nm$), showing a charge-transfer process from the pyrenecyclodextrin-SWNT hybrids to the ADA-Ru complex. Because these photoresponse processes are recoverable following the removal of the light, the present photosensor exhibits a promising application in the area of tunable light detection.

Another remarkable example of this approach was reported by the Swager group [116]. In this work, they developed an SWNT/calixarene substituted polythiophene-based resistance sensor (Fig. 11). The key point they used is that calix [4]arenes are promising receptors to differentiate the isomers of xylene because of the shape-persistent hydrophobic binding pockets of these materials in their cone conformation. Importantly, this sensor does show high sensitivity to minor structural differences in the analytes and a fast response rate. The effectiveness of this approach suggests that SWNTs dispersed in receptor-functionalized polymers are promising candidates for low-cost, real-time, and selective chemical monitoring based on host–guest chemistry.

With the increased threat of terrorist activity, there is a pressing need to develop new generations of low power, low cost, and portable sensing devices for the detection of chemical vapors indicative of malicious intent. Several groups have made great efforts towards developing SWNT-based sensing devices for detecting explosives and nerve agents [117–125]. For example, Strano and co-workers [124] employed devices composed of mostly metallic SWNTs ordered with alternating-current dielectrophoresis as chemical sensors for the detection of DMMP and $SOCl_2$. Cattanach et al. [123] reported the design of a flexible sensor, composed of SWNT bundles deposited onto a polyethylene terephthalate (PET) polymer film, for the detection of DMMP and DIMP. Johnson and co-workers [121,122] took a unique approach to chemical vapor sensing in that they used DNA-functionalized SWNTs as the sensing element and conduction channel in NTFET devices. To further improve the sensitivity and detection limit, the inte-

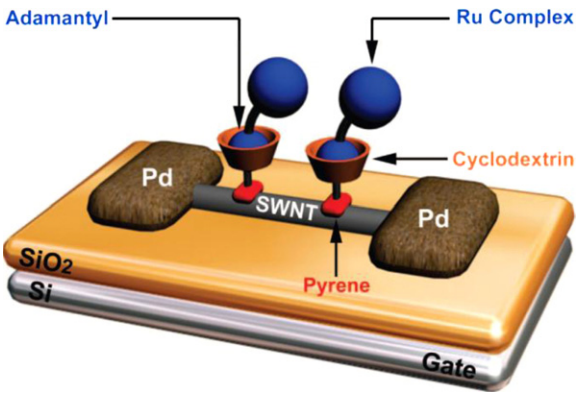

Fig. 10. A model of the pyrenecyclodextrin-decorated NTFET device showing how the pyrenecyclodextrin molecules interact with the SWNT and, at the same time, bind with guest molecules. The graphic is reproduced from ref. [115] with permission from the copyright holder.

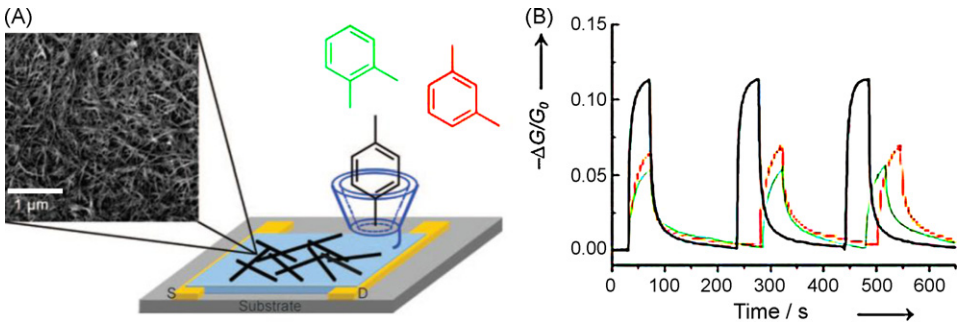

Fig. 11. (A) Schematic view of the SWNT/calixarene substituted polythiophene sensor that selectively adsorbs p-xylene. (B) Conductance change of the sensors exposed to xylene isomers (400 ppm). Black: p-xylene, green: o-xylene, red: m-xylene for all plots. These graphics are reproduced from ref. [116] with permission from the copyright holder.

gration of molecular recognition into their structures is attractive. Most recently, the Swager group developed a high-performance polymer/SWNT chemical sensor using a very simple spin-casting technique (Fig. 12) [125]. They used hexafluoroisopropanol-substituted polythiophene (HFIP-PT) or poly(3-hexylthiophene) (P3HT) to non-covalently functionalize SWNTs because of its H-binding with phosphate esters that are common to a number of chemical warfare agents. As shown in Fig. 12, the sensor response is fast and reproducible even at low analyte concentrations. The dispersing polymer provides increased sensitivity due to strong H-bonding interactions with the analyte. The effectiveness of this approach suggests that carbon nanotubes dispersed with receptor containing polymers are a promising approach for the production of low cost chemoresistive sensors [126,127].

4.5. Other functional sensors

The detection of vapor or gas species in atmosphere or process gases, using miniature and portable gas sensors that are able to detect the analytes in real time with good sensing performance, is of great importance in relation to environmental pollution, industrial emission monitoring and process control, medical diagnosis, public security, agriculture and a variety of industries. As discussed above, SWNTs are composed entirely of surface atoms, which is ideal for the direct electrical detection of trace chemical vapors where SWNTs act as both sensing materials and transducer. The

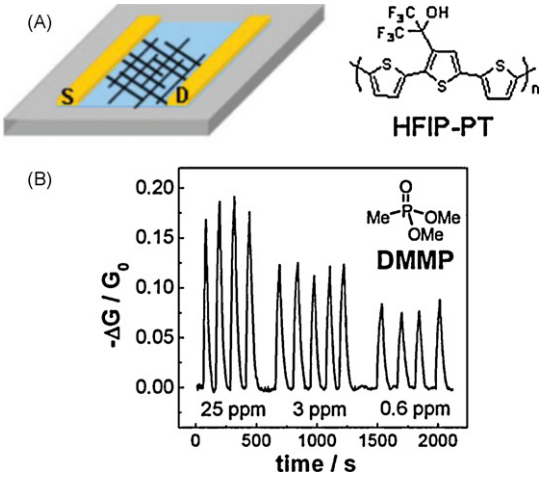

Fig. 12. (A) Schematic view of the device consisting of a percolative network of carbon nanotubes between two gold electrodes deposited by casting a HFIP-PT stabilized dispersion. (B) Conductance change ($-\Delta G/G_0$) of the sensor upon exposure to varying concentrations of DMMP. The bias voltage is fixed at 0.1 V, and the temperature is 70 °C. These graphics are reproduced from ref. [125] with permission from the copyright holder.

first paper showing the great potential of NTFETs for gas sensing applications was published in 2000. In this paper, Kong et al. [128] at Stanford University observed that a single SWNT used as a transistor channel between two gold electrodes, fabricated on a SiO_2/Si substrate acting as a bottom gate, interacted with gas molecules, changing the NTFET transfer characteristics. This work led to an explosion of both experimental and theoretical work. To date, great efforts have been made for fabricating NTFETs that show the sensitivity towards such gases as NH_3, NO_2, H_2, CH_4, CO, SO_2, H_2S, alcohols, and O_2. However, using pristine CNTs as sensing elements generally lacks specificity to different gaseous analytes and the high sensitivity towards analytes that have no affinity to SWNTs. These shortcomings can be in part circumvented by functionalizing the SWNTs with analyte-specific entities. Considering the limit of space and references, we will highlight several recent progresses for demonstrating the concept of the design, fabrication, and electrical properties of NTFET-based gas sensors. There are several good previous review papers in the literature including the reports by Kauffman, Zhang, and Bondavalli [11,129,130].

For example, Qi et al. [131] showed non-covalent functionalization of NTFETs by drop-coating polyethyleneimine (PEI) and Nafion (a polymeric perfluorinated sulfonic acid ionomer) onto devices, producing gas sensors with improved sensitivity and selectivity for NO_2 and NH_3 [132–134]. Star et al. [135] also fabricated non-covalently functionalized NTFETs by simply submerging nanotube network FETs in an aqueous solution of PEI and starch. PEI–starch polymer-coated NTFETs had n-type characteristics and were used as CO_2 gas sensors because the amine groups of polymer PEI can react with dissolved CO_2 to form carbamates with the aid of starch, which introduce scattering centers that decrease the electrical resistance in the SWNTs [136]. To detect NO in exhaled breath, Kuzmych et al. [137] developed NTFET-based sensors similarly based on PEI non-covalently functionalized SWNT networks. The detection mechanism was based on the combination of an Ascarite scrubber (to remove the interference from CO_2), a CrO_3 converter (to oxidize NO to NO_2) and conductivity measurements [138].

Another set of good examples with the best sensitivity to NO_2 and NH_3 have been reported by the Haddon group and others [139–145]. In the initial work, the Haddon group covalently functionalized NTFET devices with the polymer poly(m-aminobenzene sulfonic acid) (PABS) [139,140]. Such materials offer great promise as sensors because the attached functionality may be tailored for specific analytes while the influence of the chemistry on the oligomer side-chain is detected via a change in the electronic conductivity due to a modulation of the joint density of states of the SWNT graft-copolymer. The SWNT–PABS devices showed n-type behavior and significant sensitivity to 5 ppm NH_3. In addition to that, they also demonstrated that this was the first functionalized SWNT material with a hybrid electronic structure which is not a simple sum of the individual components [141]. Further

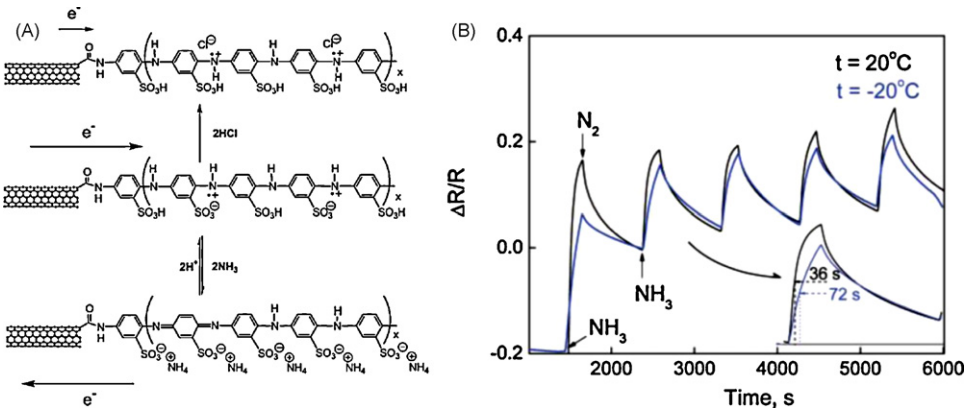

Fig. 13. (A) Schematic of the protonation/deprotonation of SWNT-PABS upon interaction with HCl and NH_3, respectively. (B) Response curves of a SWNT-PABS film to 20 ppm ammonia at 20 °C (black curves) and −20 °C (blue curves). The inset shows the delay in the response at lower temperature. These graphics are reproduced from ref. [142] with permission from the copyright holder.

work from the same group then provided definitive evidence for the mechanism of electronic detection of ammonia by monitoring *in situ* changes in the electrical resistance and optical spectra of films of poly(m-aminobenzenesulfonic acid)-functionalized SWNTs (SWNT-PABS) [142]. The increase of resistance during exposure to ammonia is associated with deprotonation of the PABS side chain that in turn induces electron transfer between the oligomer and the valence band of the semiconducting SWNTs (Fig. 13). Near IR spectroscopy was also used to demonstrate that the charge transfer is a weakly driven process, and this accounts for the high reversibility of the sensor. Following this work, Zhang et al. [143,144] used SWNT–PABS devices to achieve detection limits of 100 ppb NH_3 and 20 ppb NO_2 with short response time and total recovery. The response of the SWNT–PABS sensor to NO_2 was explained through protonation of the PABS polymer, which is logically opposite to the mechanism described for NH_3 detection. Furthermore, Li et al. [145] reported the fabrication of another SWNT sensor functionalized by poly(methyl methacrylate) (PMMA) for NH_3 detection that excluded the effects of relative humidity.

5. Inorganic materials-functionalized NTFET devices

Inorganic materials exhibit a broad range of electronic, chemical and physical properties that are often highly sensitive to changes in their chemical environment. They can be mechanically and chemically robust and stable, and hence, compared to organic materials-functionalized sensors, inorganic materials-functionalized sensors can work under harsher conditions. On the other hand, the high surface area of SWNTs and the fact that all of the carbon atoms in the SWNTs are surface atoms makes them an ideal candidate as supports for inorganic materials, in spite of the low reactivity of sp^2 hybridized C atoms. The substrates for supporting these materials have a considerable influence on their morphology and properties. Consequently, the combination of SWNTs with inorganic materials could afford functionalized NTFET sensors with the improved sensitivity and selectivity [11,29,129]. Several research groups have explored the decoration of NTFETs with different catalytic metal nanoparticles (Pd, Pt, Au, Rh, etc.) to develop specific sensors for detecting the trace chemical vapors, such as H_2, CH_4, NO_2, NH_3, CO, HCN, HCl, Cl_2, acetone, benzene, and H_2S, by means of electron-beam lithography [146,147], thermal evaporation [148], sputter-coating [148–151], drop-coating [152], chemical functionalization [150,153], and electrodeposition [147,154–156].

Among inorganic materials, semiconductor nanoparticle-SWNT hybrids have been the subject of recent interest because such hybrids are well suited for use in optoelectronic devices, given the tunable bandgap of nanoparticles and the ease of chemical fabrication [11,29,129,157–159]. Based on this concept, NTFET devices have been widely used to build functional optoelectronic devices. For example, the Stoddart group [160] used network transistors to study the charge transfer (CT) from self-assembled pyrene-functionalized CdSe (pyrene/CdSe) nanoparticles on CVD-grown SWNTs (Fig. 14). The surfaces of CdSe nanoparticles were functionalized with a pyrene derivative. The pyrene units attached to the surface of the CdSe nanoparticles associated with the surfaces of SWNTs by means of π–π interactions to facilitate the formation of the pyrene/CdSe-SWNT hybrids. The experimental results demonstrated effective CT from pyrene/CdSe nanoparticles to SWNTs by using both fluorescence quenching experiments and transistor measurements. The SWNTs act as electron acceptors and the pyrene/CdSe nanoparticles act as electron donors. The magnitude of the CT shows a strong dependency on the light intensity and wavelength and reaches a maximum of 2.2 electrons per pyrene/CdSe nanoparticle.

To mimick functions of the biological systems such as photosynthesis and vision, we employed photoactive highly crystalline, monodisperse anatase TiO_2 quantum dots to produce functional

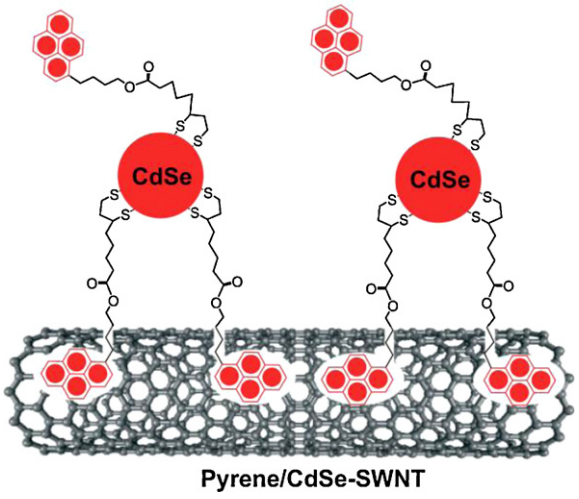

Fig. 14. Schematic drawing of the non-covalent bonding between surface-functionalized CdSe nanoparticles and a SWNT. The graphic is reproduced from ref. [160] with permission from the copyright holder.

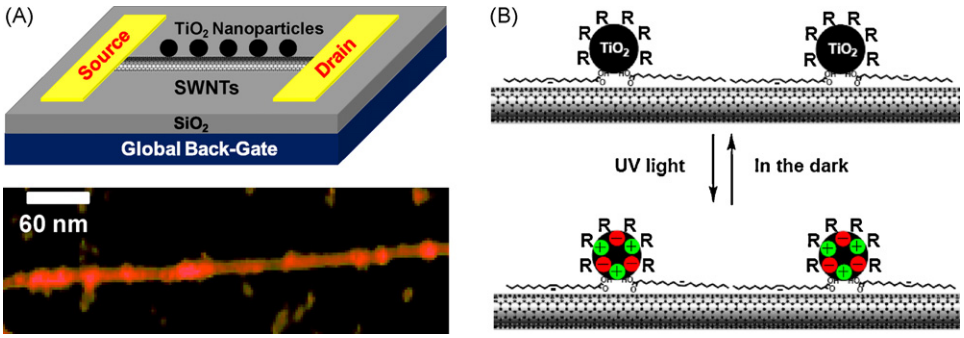

Fig. 15. (A) A schematic of SWNTs coated by TiO_2 nanoparticles and an AFM image of a representative single tube on a silicon wafer assembled by TiO_2 nanoparticles. The tube is ~2.5 nm in diameter. The average diameter of TiO_2 nanoparticles is ~ 3.6 nm. (B) Illustration of how TiO_2 nanoparticles effect the device characteristics under UV irradiation and in the dark. These graphics are reproduced from ref. [161] with permission from the copyright holder.

devices formed from individual NTFETs (Fig. 15A) [161]. The unique feature of TiO_2 nanoparticles used in this study is that UV irradiation generates free electrons (e^-) and holes (h^+) as the active centers on the nanocrystal surface (Fig. 15B). TiO_2 nanoparticles with 3–5 nm in diameter were derivatized with oleic acid because the long alkane chain of oleic acids can non-covalently associate with the surface of carbon nanotubes and therefore act as anchors to hold the photoactive TiO_2 nanoparticles close to the tube surface [49,51,94]. High-resolution atomic force micrograph (AFM) as well as Raman spectroscopic studies, thermogravimetric analysis, and high-resolution transmission electron microscope experiments proves the successful assembly of TiO_2 nanoparticles on the tube surface (Fig. 15A).

Importantly, once TiO_2 nanoparticles are tethered to the surface of the tubes, we observed reversible, fast, and significant changes in R_{on} when the devices were under UV irradiation versus in the dark. To rule out the possibility of Schottky barrier modification at the junctions between the metal electrodes and the carbon nanotube, we fabricated NTFETs with these junctions covered by an insulating layer (polymethylmethacrylate, PMMA), which was patterned using electron beam lithography. We observed essentially the same photoswitching effect after treatment of TiO_2 nanoparticles. We proposed that during UV illumination, the free electrons generated by photoinduced charge separation migrate to the surface of quantum dots, producing scattering sites for the hole carriers flowing through the tubes. These active sites can scatter the hole carriers and therefore lower the mobility in the p-type semiconducting devices. Based on this hypothesis, it can be inferred that one should observe both the hole current decrease and the electron current increase in a same device when an ambipolar material is used. As shown in Fig. 16, we observed a fast, significant current decrease when the negative gate bias was held and on the contrary, a fast large current increase under UV irradiation in the same device when the positive gate bias was applied. It is remarkable that the photoactivity of TiO_2 realizes a symmetric, opposite, "mirror image" photoswitching effect in the same device (Fig. 16).

For practical applications, increasing the photosensitivity, response speed, and selectivity of UV photodetectors is a prerequisite. To this end, we recently developed a method for fabricating tunable hybrid photodetectors (whose responsivity is as high as five orders of magnitude) by surface-functionalization of SWNTs as test-beds with high-crystal-quality zinc oxide (ZnO) nanoparticles as antennas for UV detection [162]. The special properties of ZnO nanoparticles used in this work are the large surface-to-volume ratio for the purpose of increasing the number of the surface trap states and the reduced low-dimensionality for the purpose of confining the active area of charge carrier. Due to the photoinduced adsorption and desorption of oxygen from the nanoparticle surface, the devices show the significant photoswitching effects with good reversibility and reproducibility (Fig. 17). Because ZnO nanoparticles show the wavelength-dependent photosensitivity, the devices exhibit the wavelength-dependent conductance. These exciting findings could greatly speed the application of ZnO nanomaterials for UV detection [163–167].

Rutile-structured tin oxide (SnO_2) is an n-type semiconducting material widely used in gas-sensing applications. The combination of SWNTs with continuous SnO_2 films have realized the room-temperature gas sensors for detecting NO_2, NH_3, H_2, or CO [157,158,168–170], but the fully encapsulated SWNT cannot directly participate in gas sensing, and thus, the sensitivity of the sensor is not maximized. To improve the sensitivity, most recently, Lu and Ocola [171] have demonstrated a miniaturized gas sensor using hybrid nanostructures consisting of discrete SnO_2 nanocrystals supported on multi-walled carbon nanotubes (MWNTs). In contrast to the high-temperature operation required for SnO_2 nanocrystals alone and to the insensitivity to

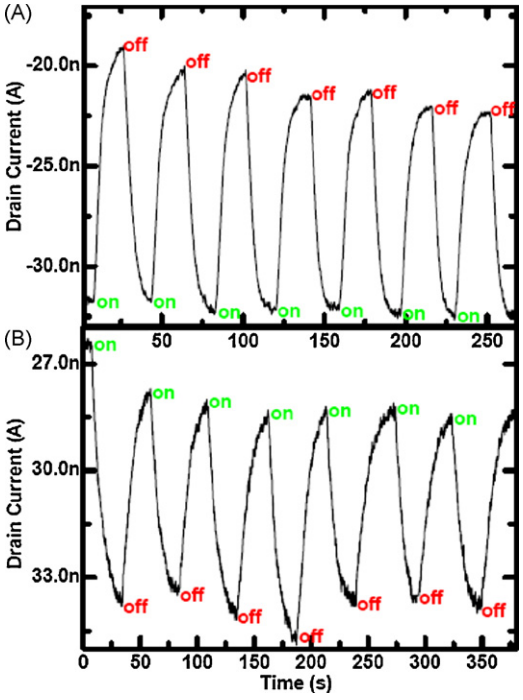

Fig. 16. Time courses of the drain current of an ambipolar device after assembly while UV light is toggled on and off. (A) The source-drain bias is −5 mV. The gate bias is −9 V. (B) The source-drain bias is 5 mV. The gate bias is 2 V. The graphic is reproduced from ref. [161] with permission from the copyright holder.

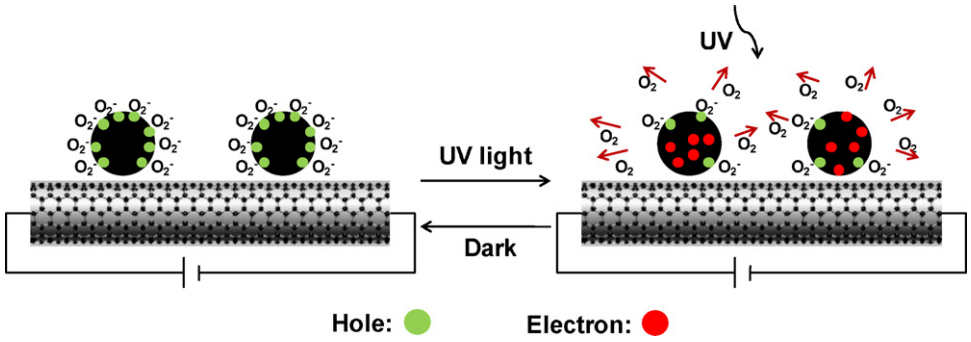

Fig. 17. Illustration of how ZnO nanoparticles affect the device characteristics under UV irradiation and in the dark. To clearly demonstrate the mechanism, we remove dodecanoic acids at the surface of ZnO nanoparticles, which are used to hold ZnO nanoparticles close to the tube surface. The graphic is reproduced from ref. [162] with permission from the copyright holder.

H_2 and CO for SWNTs alone, the hybrid SnO_2–MWNT sensor exhibited room-temperature sensing capability when exposed to low-concentration gases (NO_2, H_2, and CO). The sensing performance of the hybrid nanostructure sensor could be attributed to the effective electron transfer between SnO_2 nanocrystals and MWNTs and to the increase in the specific surface area of hybrid nanostructures (Fig. 18). This new sensing scheme will be instrumental for the development of new sensors based on hybrid nanostructures for a wide range of innovative applications.

Another interesting application of NTFETs is magnetic detecting with single-molecule sensitivity, which can offer a viable long-sought readout of magnetic information stored in individual single-molecule magnets (SMMs). To date, however, the chemistry needed to bridge the domains of carbon nanotubes and SMMs has remains unexplored. To achieve single-molecule-magnet carbon nanotube hybrids, Bogani et al. [172] fabricated the first SWNT–SMMs hybrids containing intact pyrene-functionalized SMMs in conditions compatible to the creation of electronic devices. By controlling the grafting of SMMs down to a single molecule level, they demonstrated the single-SMM sensitivity of NTFETs. These results pave the way to the construction of "double-dot" molecular spintronic devices, where a controlled number of nanomagnets are coupled to an electronic nanodevice, and to the observation of the magneto-Coulomb effect. In addition, the approach may be extended to produce different functional hybrids incorporating charge-transfer complexes, valence tautomers, or photomagnetic materials.

6. Biological materials-functionalized NTFET devices

Current techniques for biosensing typically rely on optical spectroscopy, mass spectroscopy, and gel electrophoresis that are inherently complex, low-throughput, and expensive. Although the techniques are highly sensitive and specific, it is more difficult to miniaturize. Consequently, ideally one would want a promising analytical platform which is simple, cost-effective, and requires no external modification on the biomolecules. Electronic detection techniques may offer an alternative, but their potential has not yet been explored fully. In particular, NTFETs fabricated using semiconducting SWNTs are good candidates for biosensing because of the biocompatibility and size compatibility of carbon nanotubes [17–19,38,173,174]. For example, the Dai group first developed the controlled and nanotube-specific method for immobilizing protein and small biomolecules onto non-covalently functionalized SWNTs and then investigating specific protein–protein interactions [49,51]. The Grüner group used polymer-functionalized NTFETs as testbeds for detecting the charge transfer from adsorbed proteins to SWNTs and the specific protein binding [175,176]. Following these reports, several groups modified NTFETs by more specific small biomolecules as recognition elements, such as aptamer and antibody, to develop label-free biosensors for detecting thrombin [177], prostate-specific antigen [178], and target immunoglobulin [179,180]. Single-stranded species of both deoxyribonucleic (ss-DNA) and ribonucleic acids (ss-RNA) represent a class of materials known to strongly interact with SWNTs through π–π stack-

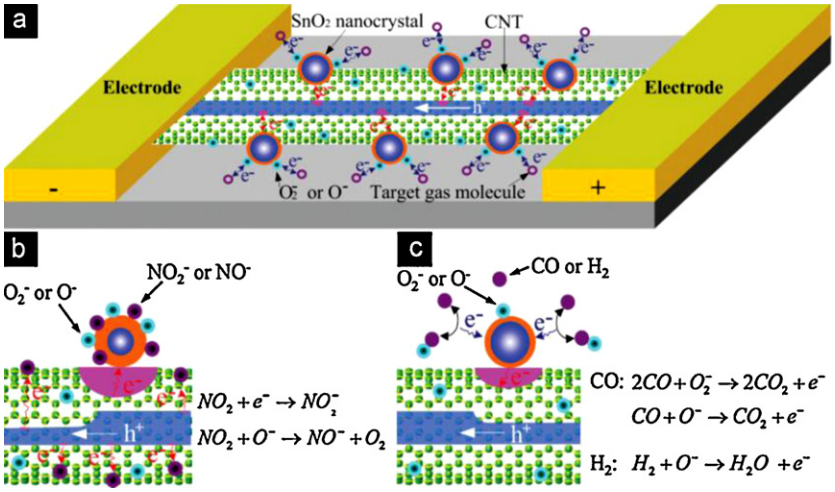

Fig. 18. (A) Discrete SnO_2 nanocrystals supported on an individual MWNT used as a new gas-sensing platform. Possible gas sensing mechanisms include (B) direct adsorption of target gas molecules (e.g., NO_2) onto the SnO_2–CNT surface inducing electron transfer and changing the sensor conductivity and C) catalytic reaction between target gas molecules (e.g., H_2 and CO) and oxygen adsorbates releasing electrons back into the SnO_2–CNT surface and changing sensor conductivity. These graphics are reproduced from ref. [171] with permission from the copyright holder.

ing. Recent experiments have already shown that NTFETs with immobilized DNAs offered a remarkable set of technologically useful properties such as chemical sensing and detection of DNA hybridization [65,121,181–183].

Although NTFETs-based biosensors have been extensively studied, they are still in their infancy. Before nanotube biosensors can be fully exploited for real-life applications, a clear understanding of how electrical conductance is affected by protein adsorption should be developed in order to optimize nanotube biosensor designs. As discussed earlier, the sensing mechanism of NTFET-based sensors is still a topic of debate. In general, there are two possibilities: electrostatic gating and Schottky barrier modification. To elucidate which one will dominate the sensing phenomenon, Chen et al. [50] designed chemical functionalization schemes to selectively block different components of the devices from protein adsorption, self-assembled monolayers (SAMs) of methoxy(poly-(ethylene glycol))thiol (mPEG-SH) on the metal electrodes and PEG-containing surfactants on the nanotubes (Fig. 19A). Extensive characterization revealed that electronic effects occurring at the metal-nanotube contacts due to protein adsorption constitute a more significant contribution to the electronic biosensing signal than adsorption solely along the exposed lengths of the nanotubes. This result seems proven by another two studies reported by Tang et al. [69] and Gui et al. [72] In the former case, hybridization of complementary ssDNA oligos can only happen with thiolated ssDNA coimmobilized with mercaptohexanol on the gold electrodes (Fig. 19B). In the latter case, they performed the evolution experiments of transfer characteristics (before immobilization, after immobilization and hybridization with its complementary DNA) for the capped NTFETs with the junction or channel exposed (Fig. 19C). In both cases, they demonstrated that DNA hybridization on gold electrodes, instead of on SWNT sidewalls, was mainly responsible for the acute electrical conductance change due to the modulation of energy level alignment between SWNT and gold contact. This work provides concrete experimental evidence on the effect of SWNT-DNA binding on DNA functionality, which will help to pave the way for future designing of SWNT biocomplexes for applications in biotechnology in general and also DNA-assisted nanotube manipulation techniques.

Byon and Choi [71] have fabricated highly sensitive network NTFET devices that have successfully detected both nonspecific adsorptions of proteins and specific protein–protein interactions at 1 pM concentrations. The increased sensitivity is mainly accredited to the increased thin and wide Schottky contact area (Fig. 20A), which has been achieved by evaporating electrode metals using a shadow mask on a tilted angle sample stage. Abe et al. [184] used an insulator-covered carbon nanotube field-effect transistor with a top-gate structure to achieve high-stability sensing of proteins of pig serum albumin (PSA) with a sensitivity limit down to 5 nM. Dong et al. [185] have carefully demonstrated a significant sensitivity enhancement in electrical detection of DNA hybridization in NTFETs by introducting reporter DNA–AuNP conjugates in the hybridization step (Fig. 20B). The amplified change in drain current allows us to reliably determine the DNA concentration down to as small as ca. 100 fM. They claimed that with detection limits in the femtomolar range, NTFET-based biosensors and immunosensors may be adapted to detection of a variety of biomarkers for applications ranging from molecular diagnostics to in vitro diagnostics.

However, the detection mechanism of NTFET-based sensors is still controversial. A very recent report from the Dekker group [186] found that electrostatic gating and Schottky barrier effects are the two relevant mechanisms based on extensive protein-adsorption experiments, with electrostatic gating being most reproducible. If the contact region is passivated, sensing is shown to be dominated by electrostatic gating, which demonstrates that the sensitive part of a nanotube transistor is not limited to the contact region, as previously suggested above. Such a layout is reasonable and provides a reliable platform for biosensing with nanotubes.

7. In-line functionalization for NTFET devices

In the scenario of device miniaturization motivated by the limits of the inherent quantum effects of conventional silicon-based devices, creating efficient optoelectronic devices using individual functional molecules is one of the ultimate goals in nanotechnology [5,22,23,76]. The development of reliable techniques for producing

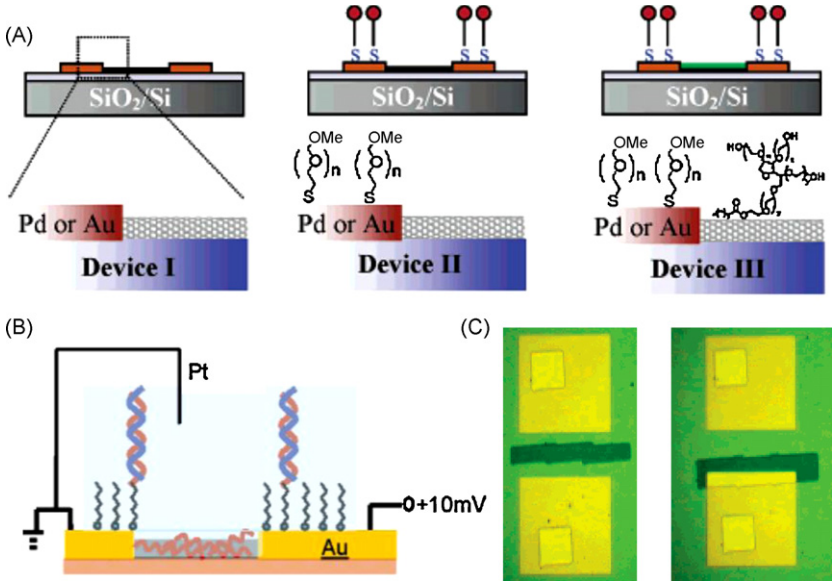

Fig. 19. (A) Three types of NTFET devices used in ref. [50]. A regular device comprised of metal contact with multiple SWNT connections is prepared by lift-off the photoresist layer immediately after metal evaporation (device type I). Formation of mPEG-SH SAM followed by lift-off affords device type II. Further treatment of type II devices with a Tween 20 solution leads to device type III. (B) Schematic illustration of a single device during electrical measurement. Complementary ssDNA oligos only hybridized to thiolated ssDNA coimmobilized with mercaptohexanol on the gold electrodes. (C) Optical images of photoresist capped Au-contacted NTFETs with one junction exposed (left) and a channel exposed (right). These graphics are reproduced from ref. [50], [69], and [72] with permission from the copyright holder.

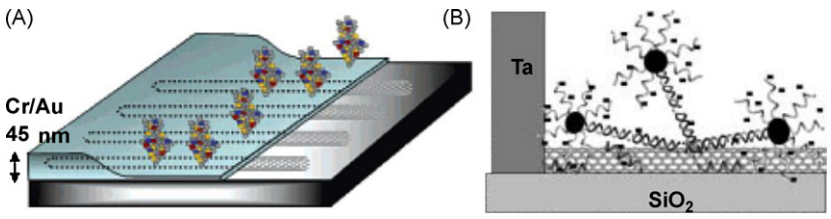

Fig. 20. (A) A view of a device with a thin and wide Schottky contact area formed by evaporating electrode metals using a shadow mask on a tilted angle sample stage. (B) Schematic illustration of DNA detection enhancement by reporter DNA–Au nanoparticle conjugates, showing the possible molecular binding on SWNTs. These graphics are reproduced from ref. [71] and [185] with permission from the copyright holder.

single molecule devices is of crucial importance to both the fundamental scientific research for probing the intrinsic properties of materials at the molecular level and rising technical demands of modern information society (such as high-speed capability, high degree of integration, high-capacity performance, and low-power consumption). However, it is difficult to build single molecule devices through chemical functionalization of the sidewalls of SWNTs. To this end, Goldsmith et al. [36] recently developed an electrochemical modification approach to point-functionalize SWNTs. By controlling the chemistry through electronically controlled electrochemical potentials, they were able to achieve single chemical attachments. This method is valuable and might find the potential applications in single molecule switching or sensing.

By taking advantage of the chemical, physical, and mechanical properties of SWNTs, we developed a reliable lithographic in-line functionalization of NTFETs to build single molecule devices based on SWNTs as point contacts (Fig. 21) [5,187,188]. To form SWNT electrodes, we started by preparing an array of SWNT transistors. Then by using ultrahigh-resolution electron-beam lithography and precise oxygen plasma ion etching, we cut the nanotubes into two half-ends with nanogaps in the range of less than 10 nm. This cutting process creates carboxylic acid endgroups on the half-tubes, which allows us to do the subsequent connection chemistry. Finally, we covalently wired the different conjugated molecular wires having the requisite amine functionality into precisely-cut SWNT nanogaps, thus leading to the formation of single molecule devices. The chemical contacts provided by amide-linked molecular bridges are robust and can tolerate broad changes in environment. This provides us with the opportunity to install capabilities into the electrical devices that are inherent to the synthetic molecular backbones. Functionality can be installed in the molecular backbone that allows the creation of pH-, redox-, and photo-gated switches, as well as metal ion recognition devices [187,189]. Furthermore, this method allows for the assembly of multicomponent structures, which offers devices that are sensitive to external inputs [76,190,191], protein/substrate binding [192], and DNA hybridization [193].

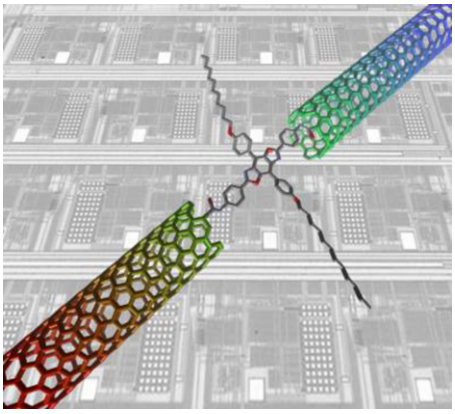

Fig. 21. Schematic demonstration of holistic construction of a single molecule circuit. The graphic is reproduced from ref. [5] with permission from the copyright holder.

7.1. Single-molecule switches

In this study, we reconnected the cut SWNTs with photochromic molecules in order to assay their ability to reversibly toggle between two distinct conductive states in response to external triggers [189]. Diarylethenes switch between open (non-conjugated) and closed (conjugated) states (Fig. 22A) and have been installed into single molecular devices with gold contacts [194,195]. We used two kinds of photochromic diarylethenes, **1** and **2** in Fig. 22A. In each of these molecules the reversible interconversion between the two states causes the rearrangement of the covalent bonds such that π-bond conjugation (and therefore the electrical conductivity) through the molecule can be switched on and off. As expected, we found that both semiconducting and metallic devices bridged with **1** showed one-way switching of the associated molecule from the lower conductance state to the higher conductance state upon exposure to UV light (365 nm) due to large extension of π-conjugation in the molecular backbone (Fig. 22B). Unfortunately, **Closed-1** was unable to revert back to the open state photochemically, which is opposite to the phenomenon observed in the devices made with dithiolated molecules within gold-electrode

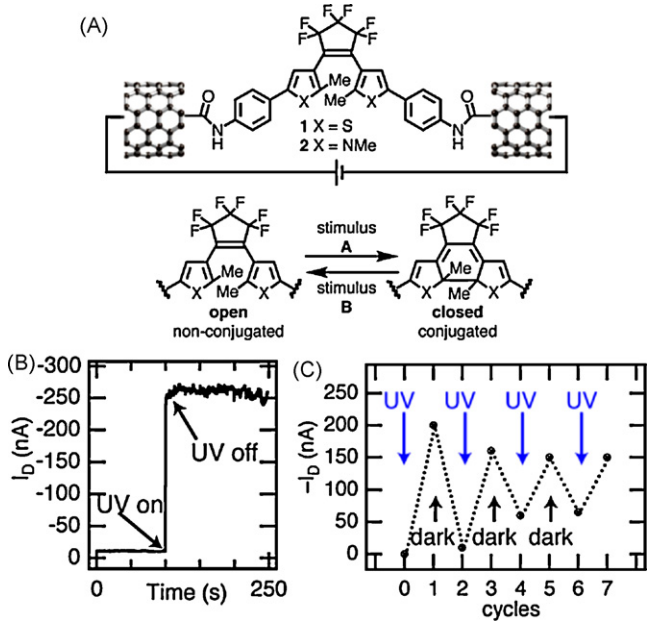

Fig. 22. (A) Molecular bridges between the ends of an individual SWNT electrode. (B) Drain current as a function of time for a device rejoined by **1**. (C) Drain current as a function of the switching cycle as the device rejoined by **2** is irradiated with UV light and then left in the dark for 12 h. These graphics are reproduced from ref. [189] with permission from the copyright holder.

break junctions [195]. To achieve reversible switching, we decided to use pyrrole-based molecule **2**, which shows the thermal back-conversion, to rejoin the devices. Similarly, with UV irradiation the bridge cyclizes after reconnection, resulting in the significant current increases. Remarkably, the low-conductance state was restored when the device was aged at room temperature overnight, and the on/off cycle can be toggled many times (Fig. 22C). This design concept, which significantly extends the clear example of thermally reversible photoswitching of single-molecule devices, provides a deeper understanding of the interplay between molecular structure, electrode materials, and emergent functions at the nanoscale level, promising the potential of applications in future nanodevices.

7.2. Single-molecule biosensors

One key advantage of this approach to molecular sensing is the ability to form a well-defined linkage between a molecular wire and SWNT electrodes. Furthermore, because it is constructed from a single molecule, each device has the capacity to monitor individual binding events. This methodology demonstrates an attractive connection between electrical conduction and biology. Our initial work using this technique in biosensing is to develop bioassay techniques by using bridge molecules with functional side groups capable of subsequent biocompatible assembly. We have been able to form complex multicomponent nanostructures from single-molecule SWNT-based devices by combining programmed chemical reactivity and directed self-assembly [192].

Following this work, we have used the method of creating multicomponent electronic devices to measure the conductivity of a single DNA duplex, which is an area of substantial interest [193]. We modified DNA sequences with amines on their termini and coupled these to the SWNT electrodes through amide linkages. Two different device connectivities were explored. In one case, we modified each of the 5′ ends of a DNA duplex and use this to bridge the SWNT gap. In a second case, we functionalized both the 3′ and 5′ ends of a single strand of DNA to allow us to measure the electrical properties of complementary and mismatched strands. In both cases the reconnected carbon nanotube devices recovered their original electrical characteristics (p-type semiconducting or metallic). Based on the statistical measurements, well-matched duplex DNA in the gap exhibits an average resistance on the order of 1 MΩ. Interestingly, a single GT or CA mismatch in a DNA 15-mer increased the resistance of the duplex ~300 fold relative to a well matched one due to the perturbations in stacking of aromatic base pairs in the core. Importantly, one DNA sequence oriented within this gap was also a substrate for *Alu* I, a blunt end restriction enzyme, which cuts the DNA, eliminating the conductive path (Fig. 23). Thus the well matched DNA assembled between SWNT electrodes maintains its native conformation when bridging the ends of the SWNTs. These results suggest that DNA molecules bridging nanodevices can serve as uniquely powerful reporters to transduce biochemical events into electrical signals at the single molecule level.

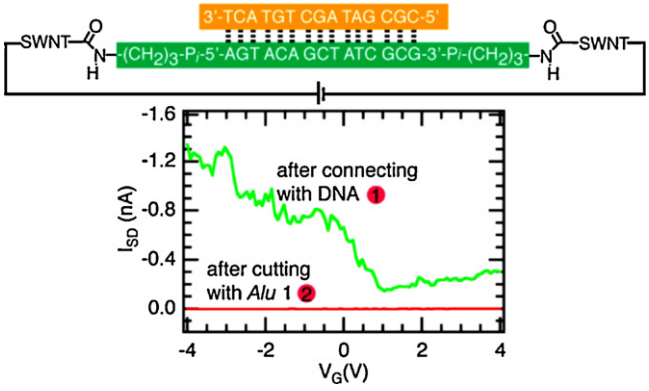

Fig. 23. Source-drain current versus gate voltage at a constant source-drain voltage (50 mV) for a metallic SWNT device after cutting and reconnection with the DNA sequence shown before (green curve: 1) and after reaction with *Alu* 1 (red curve: 2) The graphics is reproduced from ref. [193] with permission from the copyright holder.

8. Conclusions

Recent advances in chemical functionalization of NTFETs as switches and sensors are presented. SWNTs are regarded as ideal nanomaterials for integration into a variety of optoelectronic devices. At the most fundamental level, extensive work has been done through covalent or non-covalent functionalizations of SWNTs for the purpose of installing functionalities in devices capable of converting external stimuli (such as chemical, electrochemical, and photonic inputs) to easily detectable electrical signals. Moreover, NTFET devices have shown the promising future in label-free detection of the biological activities of biological molecules, even at the single molecular level, which might aid the fast development of biosensing and molecular diagnosis. Consequently, the unique feature of chemical flexibility and ultrasensitivity of SWNTs suggests that NTFET devices could serve as a platform technology for the development of new generations of compact, low-power, low-cost, and portable sensing devices with desired functionalities.

However, the exact sensing mechanism of NTFET sensors is still controversial. Although considerable attention has been devoted to the mechanistic origins of NTFET responses, it is logically very difficult to distinguish between two major mechanisms (electrostatic gating and Schottky barrier modification) since the devices must be a combination of both. To inhibit signals from less consistent metal work function modulation, contact-passivated devices formed from a single or few SWNTs might provide a reliable platform for detecting and sensing applications. A deeper fundamental understanding of the device responses to external stimuli is extremely important because it is helpful for researchers to design and develop optimized sensors.

Although much has been done about the fundamental research of NTFET sensors, and the research in this area is expanding swiftly, NTFET sensor technology is still in its early stage and many of the remaining challenges are large. For practical applications, increasing the sensitivity, response speed, and selectivity is a prerequisite. Scientists and engineers from diverse backgrounds need to come together to explore and develop new optimized sensors by combining the precise selection of molecular materials and molecular self-assembly with sophisticated device micro/nanofabrication. Another formidable issue in NTFET sensor technology is a great shortage of efficient integration strategies. Predictably, the next generation of devices would be an integrated sensor array enabling multiplexed real-time detections of analytes. In any case, the future of NTFET sensor technology looks promising, and more exciting developments in this field are expected in the future.

Acknowledgements

We acknowledge primary financial support from FANEDD (No. 2007B21), MOST (2009CB623703 and 2008AA062503), NSFC (Grant No. 50873004, 50821061, and 20833001), and Peking University.

References

[1] P. Avouris, Acc. Chem. Res. 35 (2002) 1026.
[2] H. Dai, Acc. Chem. Res. 35 (2002) 1035.
[3] M. Ouyang, J.-L. Huang, C.M. Lieber, Acc. Chem. Res. 35 (2002) 1018.

[4] S.W. Thomas III, G.D. Joly, T.M. Swager, Chem. Rev. 107 (2007) 1339.
[5] A.K. Feldman, M.L. Steigerwald, X. Guo, C. Nuckolls, Acc. Chem. Res. 41 (2008) 1731.
[6] L. Zang, Y. Che, J.S. Moore, Acc. Chem. Res. 41 (2008) 1596.
[7] J. Zhao, A.O. Pinchuk, J.M. McMahon, S. Li, L.K. Ausman, A.L. Atkinson, G.C. Schatz, Acc. Chem. Res. 41 (2008) 1710.
[8] S.-J. Park, T.A. Taton, A. Mirkin Chad, Science 295 (2002) 1503.
[9] S.E. Skrabalak, J. Chen, Y. Sun, X. Lu, L. Au, C.M. Cobley, Y. Xia, Acc. Chem. Res. 41 (2008) 1587.
[10] P.K. Jain, X. Huang, I.H. El-Sayed, M.A. El-Sayed, Acc. Chem. Res. 41 (2008) 1578.
[11] D.R. Kauffman, A. Star, Angew. Chem., Int. Ed. 47 (2008) 6550.
[12] F. Patolsky, G. Zheng, C.M. Lieber, Nat. Protoc. 1 (2006) 1711.
[13] F. Patolsky, B.P. Timko, G. Yu, Y. Fang, A.B. Greytak, G. Zheng, C.M. Lieber, Science 313 (2006) 1100.
[14] F. Patolsky, G. Zheng, C.M. Lieber, Anal. Chem. 78 (2006) 4260.
[15] G. Zheng, F. Patolsky, Y. Cui, W.U. Wang, C.M. Lieber, Nat. Biotechnol. 23 (2005) 1294.
[16] F. Patolsky, G. Zheng, O. Hayden, M. Lakadamyali, X. Zhuang, C.M. Lieber, Proc. Natl. Acad. Sci. U. S. A. 101 (2004) 14017.
[17] G. Gruner, Anal. Bioanal. Chem. 384 (2006) 322.
[18] D.R. Kauffman, A. Star, Chem. Soc. Rev. 37 (2008) 1197.
[19] B.L. Allen, P.D. Kichambare, A. Star, Adv. Mater. 19 (2007) 1439.
[20] E. Stern, J.F. Klemic, D.A. Routenberg, P.N. Wyrembak, D.B. Turner-Evans, A.D. Hamilton, D.A. LaVan, T.M. Fahmy, M.A. Reed, Nature 445 (2007) 519.
[21] Z.L. Wang, Adv. Mater. 19 (2007) 889.
[22] J. Robertson, Mater. Today 10 (2007) 36.
[23] S.E. Thompson, S. Parthasarathy, Mater. Today 9 (2006) 20.
[24] S. Iijima, Nature 354 (1991) 56.
[25] S.J. Tans, A.R.M. Verschueren, C. Dekker, Nature 393 (1998) 49.
[26] R. Martel, T. Schmidt, H.R. Shea, T. Hertel, P. Avouris, Appl. Phys. Lett. 73 (1998) 2447.
[27] N. Sinha, J. Ma, J.T.W. Yeow, J. Nanosci. Nanotechnol. 6 (2006) 573.
[28] J. Li, Carbon Nanotubes (2005) 213.
[29] D. Vairavapandian, P. Vichchulada, M.D. Lay, Anal. Chim. Acta 626 (2008) 119.
[30] L. Mishra, S. Dwivedi, D. Pandey, A. Dwivedi, G.S. Tomar, PharmaChem 7 (2008) 16.
[31] M. Kaur, D.K. Aswal, J.V. Yakhmi, Sci. Technol. Chemiresistor Gas Sens. (2007) 33.
[32] S.B. Jain, P. Kang, Y.-H. Yun, T. He, S.L. Pammi, A. Muskin, S. Narasimhadevara, D. Hurd, M.J. Schulz, J. Chase, S. Subramaniam, V. Shanov, F.J. Boerio, D. Shi, R. Gilliland, D. Mast, C. Sloan, Proc. SPIE-Int. Soc. Opt. Eng. 5389 (2004) 167.
[33] B.S. Sherigara, W. Kutner, F. D'Souza, Electroanalysis 15 (2003) 753.
[34] Q. Cao, J.A. Rogers, Adv. Mater. 21 (2009) 29.
[35] P. Sharma, P. Ahuja, Mater. Res. Bull. 43 (2008) 2517.
[36] B.R. Goldsmith, J.G. Coroneus, V.R. Khalap, A.A. Kane, G.A. Weiss, P.G. Collins, Science 315 (2007) 77.
[37] A. Hirsch, Angew. Chem., Int. Ed. 41 (2002) 1853.
[38] M. Prato, K. Kostarelos, A. Bianco, Acc. Chem. Res. 41 (2008) 60.
[39] D. Tasis, N. Tagmatarchis, V. Georgakilas, M. Prato, Chem. Eur. J. 9 (2003) 4000.
[40] S. Banerjee, T. Hemraj-Benny, S.S. Wong, Adv. Mater. 17 (2005) 17.
[41] S. Banerjee, M.G.C. Kahn, S.S. Wong, Chem. Eur. J. 9 (2003) 1898.
[42] J. Chen, M.A. Hamon, H. Hu, Y. Chen, A.M. Rao, P.C. Eklund, R.C. Haddon, Science 282 (1998) 95.
[43] T. Lin, V. Bajpai, T. Ji, L. Dai, Aust. J. Chem. 56 (2003) 635.
[44] D. Tasis, N. Tagmatarchis, A. Bianco, M. Prato, Chem. Rev. 106 (2006) 1105.
[45] K. Balasubramanian, M. Burghard, Small 1 (2005) 180.
[46] V.N. Khabashesku, W.E. Billups, J.L. Margrave, Acc. Chem. Res. 35 (2002) 1087.
[47] Z. Gu, H. Peng, R.H. Hauge, R.E. Smalley, J.L. Margrave, Nano Lett. 2 (2002) 1009.
[48] Y.-L. Zhao, J.F. Stoddart, Acc. Chem. Res 42 (2009) 1161.
[49] R.J. Chen, S. Bangsaruntip, K.A. Drouvalakis, N.W.S. Kam, M. Shim, Y. Li, W. Kim, P.J. Utz, H. Dai, Proc. Natl. Acad. Sci. U. S. A. 100 (2003) 4984.
[50] R.J. Chen, H.C. Choi, S. Bangsaruntip, E. Yenilmez, X. Tang, Q. Wang, Y.-L. Chang, H. Dai, J. Am. Chem. Soc. 126 (2004) 1563.
[51] R.J. Chen, Y. Zhang, D. Wang, H. Dai, J. Am. Chem. Soc. 123 (2001) 3838.
[52] D.A. Britz, A.N. Khlobystov, Chem. Soc. Rev. 35 (2006) 637.
[53] O.-K. Kim, J. Je, J.W. Baldwin, S. Kooi, P.E. Pehrsson, L.J. Buckley, J. Am. Chem. Soc. 125 (2003) 4426.
[54] A. Star, Y. Liu, K. Grant, L. Ridvan, J.F. Stoddart, D.W. Steuerman, M.R. Diehl, A. Boukai, J.R. Heath, Macromolecules 36 (2003) 553.
[55] A. Star, J.F. Stoddart, Macromolecules 35 (2002) 7516.
[56] A. Star, D.W. Steuerman, J.R. Heath, J.F. Stoddart, Angew. Chem., Int. Ed. 41 (2002) 2508.
[57] D.W. Steuerman, A. Star, R. Narizzano, H. Choi, R.S. Ries, C. Nicolini, J.F. Stoddart, J.R. Heath, J. Phys. Chem. B 106 (2002) 3124.
[58] A. Star, J.F. Stoddart, D. Steuerman, M. Diehl, A. Boukai, E.W. Wong, X. Yang, S.-W. Chung, H. Choi, J.R. Heath, Angew. Chem., Int. Ed. 40 (2001) 1721.
[59] D.M. Guldi, G.M.A. Rahman, N. Jux, N. Tagmatarchis, M. Prato, Angew. Chem., Int. Ed. 43 (2004) 5526.
[60] P.W. Barone, M.S. Strano, Angew. Chem., Int. Ed. 45 (2006) 8138.
[61] C. Ehli, G.M.A. Rahman, N. Jux, D. Balbinot, D.M. Guldi, F. Paolucci, M. Marcaccio, D. Paolucci, M. Melle-Franco, F. Zerbetto, S. Campidelli, M. Prato, J. Am. Chem. Soc. 128 (2006) 11222.
[62] H.M. Angeles, C. Ehli, S. Campidelli, M. Gutierrez, G.L. Hug, K. Ohkubo, S. Fukuzumi, M. Prato, N. Martin, D.M. Guldi, J. Am. Chem. Soc. 130 (2008) 66.
[63] D.A. Heller, E.S. Jeng, T.-K. Yeung, B.M. Martinez, A.E. Moll, J.B. Gastala, M.S. Strano, Science 311 (2006) 508.
[64] D.A. Heller, S. Baik, T.E. Eurell, M.S. Strano, Adv. Mater. 17 (2005) 2793.
[65] P.W. Barone, S. Baik, D.A. Heller, M.S. Strano, Nat. Mater. 4 (2005) 86.
[66] M. Zheng, A. Jagota, M.S. Strano, A.P. Santos, P. Barone, S.G. Chou, B.A. Diner, M.S. Dresselhaus, R.S. McLean, G.B. Onoa, G.G. Samsonidze, E.D. Semke, M. Usrey, D.J. Walls, Science 302 (2003) 1545.
[67] A. Star, V. Joshi, T.-R. Han, M.V.P. Altoe, G. Gruener, J.F. Stoddart, Org. Lett. 6 (2004) 2089.
[68] M.S. Dresselhaus, G. Dresselhaus, P. Avouris, Carbon Nanotubes Synthesis, Structure, Properties, and Applications, Springer-Verlag, New York, 2001.
[69] X. Tang, S. Bansaruntip, N. Nakayama, E. Yenilmez, Y.-l. Chang, Q. Wang, Nano Lett. 6 (2006) 1632.
[70] X. Cui, M. Freitag, R. Martel, L. Brus, P. Avouris, Nano Lett. 3 (2003) 783.
[71] H.R. Byon, H.C. Choi, J. Am. Chem. Soc. 128 (2006) 2188.
[72] E.L. Gui, L.-J. Li, K. Zhang, Y. Xu, X. Dong, X. Ho, P.S. Lee, J. Kasim, Z.X. Shen, J.A. Rogers, S.G. Mhaisalkar, J. Am. Chem. Soc. 129 (2007) 14427.
[73] T. Nakanishi, A. Bachtold, C. Dekker, Phys. Rev. B 66 (2002), 073307/1.
[74] M. Freitag, A.T. Johnson, S.V. Kalinin, D.A. Bonnell, Phys. Rev. Lett. 89 (2002), 216801/1.
[75] S. Heinze, J. Tersoff, R. Martel, V. Derycke, J. Appenzeller, P. Avouris, Phys. Rev. Lett. 89 (2002), 106801/1.
[76] Y. Cao, M.L. Steigerwald, C. Nuckolls, X. Guo, Adv. Mater., doi:10.1002/adma.200900504.
[77] K. Bradley, J.-C.P. Gabriel, A. Star, G. Gruener, Appl. Phys. Lett. 83 (2003) 3821.
[78] M.-J. Blanco, M. Consuelo Jimenez, J.-C. Chambron, V. Heitz, M. Linke, J.-P. Sauvage, Chem. Soc. Rev. 28 (1999) 293.
[79] J.P. Sauvage, C. Dietrich-Buchecker, Molecular Catenanes, Rotaxanes and Knots: A Journey Through the World of Molecular Topology, Wiley VCH, New York, 1999.
[80] F. Arico, J.D. Badjic, S.J. Cantrill, A.H. Flood, K.C.F. Leung, Y. Liu, J.F. Stoddart, Top. Curr. Chem. 249 (2005) 203.
[81] C.A. Schalley, K. Beizai, F. Voegtle, Acc. Chem. Res. 34 (2001) 465.
[82] J.-P. Sauvage, Acc. Chem. Res. 31 (1998) 611.
[83] X. Guo, Y. Zhou, M. Feng, Y. Xu, D. Zhang, H. Gao, Q. Fan, D. Zhu, Adv. Funct. Mater. 17 (2007) 763.
[84] A.R. Pease, J.O. Jeppesen, J.F. Stoddart, Y. Luo, C.P. Collier, J.R. Heath, Acc. Chem. Res. 34 (2001) 433.
[85] C.P. Collier, E.W. Wong, M. Belohradsky, F.M. Raymo, J.F. Stoddart, P.J. Kuekes, R.S. Williams, J.R. Heath, Science 285 (1999) 391.
[86] C.P. Collier, G. Matterstei, E.W. Wong, Y. Luo, K. Beverly, J. Sampaio, F.M. Raymo, J.F. Stoddart, J.R. Heath, Science 289 (2000) 1172.
[87] M.R. Diehl, D.W. Steuerman, H.-r. Tseng, S.A. Vignon, A. Star, P.C. Celestre, J.F. Stoddart, J.R. Heath, ChemPhysChem 4 (2003) 1335.
[88] G. Berkovic, V. Krongauz, V. Weiss, Chem. Rev. 100 (2000) 1741.
[89] N. Tamai, H. Miyasaka, Chem. Rev. 100 (2000) 1875.
[90] Q. Shen, Y. Cao, S. Liu, M.L. Steigerwald, X. Guo, J. Phys. Chem. C 113 (2009) 10807.
[91] G. Jiang, Y. Song, X. Guo, D. Zhang, D. Zhu, Adv. Mater. 20 (2008) 2888.
[92] X. Guo, Y. Zhou, D. Zhang, B. Yin, Z. Liu, C. Liu, Z. Lu, Y. Huang, D. Zhu, J. Org. Chem. 69 (2004) 8924.
[93] X. Guo, D. Zhang, G. Yu, M. Wan, J. Li, Y. Liu, D. Zhu, Adv. Mater. 16 (2004) 636.
[94] X. Guo, L. Huang, S. O'Brien, P. Kim, C. Nuckolls, J. Am. Chem. Soc. 127 (2005) 15045.
[95] R.F. Khairutdinov, M.E. Itkis, R.C. Haddon, Nano Lett. 4 (2004) 1529.
[96] S. Benard, P. Yu, Adv. Mater. 12 (2000) 48.
[97] J.M. Simmons, I. In, V.E. Campbell, T.J. Mark, F. Leonard, P. Gopalan, M.A. Eriksson, Phys. Rev. Lett. 98 (2007), 086802/1.
[98] X. Zhou, T. Zifer, B.M. Wong, K.L. Krafcik, F. Leonard, A.L. Vance, Nano Lett. 9 (2009) 1028.
[99] G. Yu, J. Gao, J.C. Hummelen, F. Wudl, A.J. Heeger, Science 270 (1995) 1789.
[100] A.C. Mayer, S.R. Scully, B.E. Hardin, M.W. Rowell, M.D. McGehee, Mater. Today 10 (2007) 28.
[101] V. Balzani, P. Ceroni, A. Juris, M. Venturi, S. Campagna, F. Puntoriero, S. Serroni, Coord. Chem. Rev. 219–221 (2001) 545.
[102] A. Harriman, R. Ziessel, Coord. Chem. Rev. 171 (1998) 331.
[103] J.B. Cui, R. Sordan, M. Burghard, K. Kern, Appl. Phys. Lett. 81 (2002) 3260.
[104] M. Radosavljevic, M. Freitag, K.V. Thadani, A.T. Johnson, Nano Lett. 2 (2002) 761.
[105] M.S. Fuhrer, B.M. Kim, T. Duerkop, T. Brintlinger, Nano Lett. 2 (2002) 755.
[106] A. Star, Y. Lu, K. Bradley, G. Gruener, Nano Lett. 4 (2004) 1587.
[107] D.S. Hecht, R.J.A. Ramirez, M. Briman, E. Artukovic, K.S. Chichak, J.F. Stoddart, G. Gruener, Nano Lett. 6 (2006) 2031.
[108] R.A. Hatton, N.P. Blanchard, V. Stolojan, A.J. Miller, S.R.P. Silva, Langmuir 23 (2007) 6424.
[109] B. Pradhan, K. Setyowati, H. Liu, D.H. Waldeck, J. Chen, Nano Lett. 8 (2008) 1142.
[110] M. Freitag, Y. Martin, J.A. Misewich, R. Martel, P. Avouris, Nano Lett. 3 (2003) 1067.
[111] X. Qiu, M. Freitag, V. Perebeinos, P. Avouris, Nano Lett. 5 (2005) 749.
[112] J. Borghetti, V. Derycke, S. Lenfant, P. Chenevier, A. Filoramo, M. Goffman, D. Vuillaume, J.-P. Bourgoin, Adv. Mater. 18 (2006) 2535.
[113] C. Anghel, V. Derycke, A. Filoramo, S. Lenfant, B. Giffard, D. Vuillaume, J.-P. Bourgoin, Nano Lett. 8 (2008) 3619.
[114] Y.-L. Zhao, L. Hu, J.F. Stoddart, G. Gruner, Adv. Mater. 20 (2008) 1910.

[115] Y.-L. Zhao, L. Hu, G. Gruner, J.F. Stoddart, J. Am. Chem. Soc. 130 (2008) 16996.
[116] F. Wang, Y. Yang, T.M. Swager, Angew. Chem., Int. Ed. 47 (2008) 8394.
[117] J. Li, Y. Lu, Q. Ye, M. Cinke, J. Han, M. Meyyappan, Nano Lett. 3 (2003) 929.
[118] J.P. Novak, E.S. Snow, E.J. Houser, D. Park, J.L. Stepnowski, R.A. McGill, Appl. Phys. Lett. 83 (2003) 4026.
[119] E.S. Snow, F.K. Perkins, J.A. Robinson, Chem. Soc. Rev. 35 (2006) 790.
[120] E.S. Snow, F.K. Perkins, E.J. Houser, S.C. Badescu, T.L. Reinecke, Science 307 (2005) 1942.
[121] C. Staii, A.T. Johnson Jr., M. Chen, A. Gelperin, Nano Lett. 5 (2005) 1774.
[122] A.T.C. Johnson, C. Staii, M. Chen, S. Khamis, R. Johnson, M.L. Klein, A. Gelperin, Semicond. Sci. Technol. 21 (2006) S17.
[123] K. Cattanach, R.D. Kulkarni, M. Kozlov, S.K. Manohar, Nanotechnology 17 (2006) 4123.
[124] C.Y. Lee, S. Baik, J. Zhang, R.I. Masel, M.S. Strano, J. Phys. Chem. B 110 (2006) 11055.
[125] F. Wang, H. Gu, T.M. Swager, J. Am. Chem. Soc. 130 (2008) 5392.
[126] T. Someya, J. Small, P. Kim, C. Nuckolls, J.T. Yardley, Nano Lett. 3 (2003) 877.
[127] H.J. Song, Y. Lee, T. Jiang, A.G. Kussow, M. Lee, S. Hong, Y.K. Kwon, H.C. Choi, J. Phys. Chem. C 112 (2008) 629.
[128] J. Kong, N.R. Franklin, C. Zhou, M.G. Chapline, S. Peng, K. Cho, H. Dai, Science 287 (2000) 622.
[129] T. Zhang, S. Mubeen, N.V. Myung, M.A. Deshusses, Nanotechnology 19 (2008), 332001/1.
[130] P. Bondavalli, P. Legagneux, D. Pribat, Sens. Actuators, B B140 (2009) 304.
[131] P. Qi, O. Vermesh, M. Grecu, A. Javey, O. Wang, H.J. Dai, Nano Lett. 3 (2003) 347.
[132] Y.W. Chang, J.S. Oh, S.H. Yoo, H.H. Choi, K.H. Yoo, Nanotechnology 18 (2007).
[133] D.R. Kauffman, A. Star, J. Phys. Chem. C 112 (2008) 4430.
[134] P.G. Collins, K. Bradley, M. Ishigami, A. Zettl, Science 287 (2000) 1801.
[135] A. Star, T.-R. Han, V. Joshi, J.-C.P. Gabriel, G. Gruener, Adv. Mater. 16 (2004) 2049.
[136] X.C. Dong, D.L. Fu, M.O. Ahmed, Y.M. Shi, S.G. Mhaisalkar, S. Zhang, S. Moochhala, X. Ho, J.A. Rogers, L.J. Li, Chem. Mater. 19 (2007) 6059.
[137] O. Kuzmych, B.L. Allen, A. Star, Nanotechnology 18 (2007).
[138] D.L. Fu, Y.P. Xu, L.J. Li, Y. Chen, S.G. Mhaisalkar, F.Y.C. Boey, T.W. Lin, S. Moochhala, Carbon 45 (2007) 1911.
[139] E. Bekyarova, M. Davis, T. Burch, M.E. Itkis, B. Zhao, S. Sunshine, R.C. Haddon, J. Phys. Chem. B 108 (2004) 19717.
[140] B. Zhao, H. Hu, R.C. Haddon, Adv. Funct. Mater. 14 (2004) 71.
[141] B. Zhao, H. Hu, A.P. Yu, D. Perea, R.C. Haddon, J. Am. Chem. Soc. 127 (2005) 8197.
[142] E. Bekyarova, I. Kalinina, M.E. Itkis, L. Beer, N. Cabrera, R.C. Haddon, J. Am. Chem. Soc. 129 (2007) 10700.
[143] Z. Ting, S. Mubeen, E. Bekyarova, Y. Bong Young, R.C. Haddon, N.V. Myung, M.A. Deshusses, Nanotechnology 18 (2007) 165504.
[144] T. Zhang, M.B. Nix, B.Y. Yoo, M.A. Deshusses, N.V. Myung, Electroanalysis 18 (2006) 1153.
[145] Y. Li, H.C. Wang, M.J. Yang, Sens. Actuators B 121 (2007) 496.
[146] J. Kong, M.G. Chapline, H. Dai, Adv. Mater. 13 (2001) 1384.
[147] A. Star, V. Joshi, S. Skarupo, D. Thomas, J.-C.P. Gabriel, J. Phys. Chem. B 110 (2006) 21014.
[148] J. Sippel-Oakley, H.-T. Wang, B.S. Kang, Z. Wu, F. Ren, A.G. Rinzler, S.J. Pearton, Nanotechnology 16 (2005) 2218.
[149] Y. Lu, J. Li, J. Han, H.T. Ng, C. Binder, C. Partridge, M. Meyyappan, Chem. Phys. Lett. 391 (2004) 344.
[150] I. Sayago, E. Terrado, M. Aleixandre, M.C. Horrillo, M.J. Fernandez, J. Lozano, E. Lafuente, W.K. Maser, A.M. Benito, M.T. Martinez, J. Gutierrez, E. Munoz, Sens. Actuators, B B122 (2007) 75.
[151] M. Penza, G. Cassano, R. Rossi, M. Alvisi, A. Rizzo, M.A. Signore, T. Dikonimos, E. Serra, R. Giorgi, Appl. Phys. Lett. 90 (2007).
[152] P. Young, Y. Lu, R. Terrill, J. Li, J. Nanosci. Nanotechnol. 5 (2005) 1509.
[153] M.K. Kumar, S. Ramaprabhu, J. Phys. Chem. B 110 (2006) 11291.
[154] S. Mubeen, T. Zhang, B. Yoo, M.A. Deshusses, N.V. Myung, J. Phys. Chem. C 111 (2007) 6321.
[155] Y. Lu, C. Partridge, M. Meyyappan, J. Li, J. Electroanal. Chem. 593 (2006) 105.
[156] Y. Sun, H.H. Wang, Appl. Phys. Lett. 90 (2007), 213107/1.
[157] N.D. Hoa, N. Van Quy, Y.S. Cho, D. Kim, Phys. Status Solidi A 204 (2007) 1820.
[158] Y.X. Liang, Y.J. Chen, T.H. Wang, Appl. Phys. Lett. 85 (2004) 666.
[159] C. Bittencourt, A. Felten, E.H. Espinosa, R. Ionescu, E. Llobet, X. Correig, J.J. Pireaux, Sens. Actuators, B B115 (2006) 33.
[160] L. Hu, Y.-L. Zhao, K. Ryu, C. Zhou, J.F. Stoddart, G. Gruner, Adv. Mater. 20 (2008) 939.
[161] S. Liu, J. Li, Q. Shen, Y. Cao, X. Guo, G. Zhang, C. Feng, J. Zhang, Z. Liu, M.L. Steigerwald, D. Xu, C. Nuckolls, Angew. Chem., Int. Ed. 48 (2009) 4759.
[162] S. Liu, J. Ye, Y. Cao, Q. Shen, Z. Liu, L. Qi, X. Guo, Small 5 (2009) 2371.
[163] Y. Liu, C.R. Gorla, S. Liang, N. Emanetoglu, Y. Lu, H. Shen, M. Wraback, J. Electron. Mater. 29 (2000) 69.
[164] C.S. Lao, M.-C. Park, Q. Kuang, Y. Deng, A.K. Sood, D.L. Polla, Z.L. Wang, J. Am. Chem. Soc. 129 (2007) 12096.
[165] Y. Jin, J. Wang, B. Sun, J.C. Blakesley, N.C. Greenham, Nano Lett. 8 (2008) 1649.
[166] C. Soci, A. Zhang, B. Xiang, S.A. Dayeh, D.P.R. Aplin, J. Park, X.Y. Bao, Y.H. Lo, D. Wang, Nano Lett. 7 (2007) 1003.
[167] Z. Zhang, L. Sun, Y. Zhao, Z. Liu, D. Liu, L. Cao, B. Zou, W. Zhou, C. Gu, S. Xie, Nano Lett. 8 (2008) 652.
[168] B.-Y. Wei, M.-C. Hsu, P.-G. Su, H.-M. Lin, R.-J. Wu, H.-J. Lai, Sens. Actuators, B B101 (2004) 81.
[169] L. Zhao, M. Choi, H.-S. Kim, S.-H. Hong, Nanotechnology 18 (2007), 445501/1.
[170] A. Yang, X. Tao, R. Wang, S. Lee, C. Surya, Appl. Phys. Lett. 91 (2007), 133110/1.
[171] G. Lu, L.E. Ocola, J. Chen, Adv. Mater 21 (2009) 2487.
[172] L. Bogani, C. Danieli, E. Biavardi, N. Bendiab, A.-L. Barra, E. Dalcanale, W. Wernsdorfer, A. Cornia, Angew. Chem., Int. Ed. 48 (2009) 746.
[173] S. Daniel, T.P. Rao, K.S. Rao, S.U. Rani, G.R.K. Naidu, H.Y. Lee, T. Kawai, Sens. Actuators B 122 (2007) 672.
[174] K. Balasubramanian, M. Burghard, Anal. Bioanal. Chem. 385 (2006) 452.
[175] K. Bradley, M. Briman, A. Star, G. Gruener, Nano Lett. 4 (2004) 253.
[176] A. Star, J.-C.P. Gabriel, K. Bradley, G. Gruener, Nano Lett. 3 (2003) 459.
[177] H.-M. So, K. Won, Y.H. Kim, B.-K. Kim, B.H. Ryu, P.S. Na, H. Kim, J.-O. Lee, J. Am. Chem. Soc. 127 (2005) 11906.
[178] C. Li, M. Curreli, H. Lin, B. Lei, F.N. Ishikawa, R. Datar, R.J. Cote, M.E. Thompson, C.W. Zhou, J. Am. Chem. Soc. 127 (2005) 12484.
[179] K. Maehashi, T. Katsura, K. Kerman, Y. Takamura, K. Matsumoto, E. Tamiya, Anal. Chem. 79 (2007) 782.
[180] J.P. Kim, B.Y. Lee, S. Hong, S.J. Sim, Anal. Biochem. 381 (2008) 193.
[181] A. Star, E. Tu, J. Niemann, J.-C.P. Gabriel, C.S. Joiner, C. Valcke, Proc. Natl. Acad. Sci. U. S. A. 103 (2006) 921.
[182] M. Chen, S.M. Khamis, R.R. Johnson, C. Staii, M.L. Klein, J.E. Fischer, A.T. Johnson, Mater. Res. Soc. Symp. Proc. (2007), 0963-Q21-04.
[183] S.M. Khamis, M. Chen, A.T.C. Johnson, Mater. Res. Soc. Symp. Proc. (2008) 1057E.
[184] M. Abe, K. Murata, A. Kojima, Y. Ifuku, M. Shimizu, T. Ataka, K. Matsumoto, J. Phys. Chem. C 111 (2007) 8667.
[185] X. Dong, C.M. Lau, A. Lohani, S.G. Mhaisalkar, J. Kasim, Z. Shen, X. Ho, J.A. Rogers, L.-J. Li, Adv. Mater. 20 (2008) 2389.
[186] I. Heller, A.M. Janssens, J. Maennik, E.D. Minot, S.G. Lemay, C. Dekker, Nano Lett. 8 (2008) 591.
[187] X. Guo, P. Small Joshua, E. Klare Jennifer, Y. Wang, S. Purewal Meninder, I.W. Tam, B.H. Hong, R. Caldwell, L. Huang, S. O'Brien, J. Yan, R. Breslow, S.J. Wind, J. Hone, P. Kim, C. Nuckolls, Science 311 (2006) 356.
[188] X. Guo, C. Nuckolls, J. Mate. Chem. 19 (2009) 5470.
[189] A.C. Whalley, M.L. Steigerwald, X. Guo, C. Nuckolls, J. Am. Chem. Soc. 129 (2007) 12590.
[190] X. Guo, M. Myers, S. Xiao, M. Lefenfeld, R. Steiner, G.S. Tulevski, J. Tang, J. Baumert, F. Leibfarth, J.T. Yardley, M.L. Steigerwald, P. Kim, C. Nuckolls, Proc. Natl. Acad. Sci. U. S. A. 103 (2006) 11452.
[191] X. Guo, S. Xiao, M. Myers, Q. Miao, M.L. Steigerwald, C. Nuckolls, Proc. Natl. Acad. Sci. U. S. A. 106 (2009) 691.
[192] X. Guo, A. Whalley, J.E. Klare, L. Huang, S. O'Brien, M.L. Steigerwald, C. Nuckolls, Nano Lett. 7 (2007) 1119.
[193] X. Guo, A.A. Gorodetsky, J. Hone, J.K. Barton, C. Nuckolls, Nat. Nanotechnol. 3 (2008) 163.
[194] J. He, F. Chen, P.A. Liddell, J. Andreasson, S.D. Straight, D. Gust, T.A. Moore, A.L. Moore, J. Li, O.F. Sankey, S.M. Lindsay, Nanotechnology 16 (2005) 695.
[195] D. Dulic, S.J. van der Molen, T. Kudernac, H.T. Jonkman, J.J.D. de Jong, T.N. Bowden, J. van Esch, B.L. Feringa, B.J. van Wees, Phys. Rev. Lett. 91 (2003), 207402/1.